

Second-Order Finite Difference Approximations of the Upper-Convected Time Derivative

Débora O. Medeiros*, Hirofumi Notsu[†] and Cassio M. Oishi[‡]

Abstract

In this work, new finite difference schemes are presented for dealing with the upper-convected time derivative in the context of the generalized Lie derivative. The upper-convected time derivative, which is usually encountered in the constitutive equation of the popular viscoelastic models, is reformulated in order to obtain approximations of second-order in time for solving a simplified constitutive equation in one and two dimensions. The theoretical analysis of the truncation errors of the methods takes into account the linear and quadratic interpolation operators based on a Lagrangian framework. Numerical experiments illustrating the theoretical results for the model equation defined in one and two dimensions are included. Finally, the finite difference approximations of second-order in time are also applied for solving a two-dimensional Oldroyd-B constitutive equation subjected to a prescribed velocity field at different Weissenberg numbers.

Keywords: Generalized Lie derivative, Lagrangian scheme, Finite difference method

1 Introduction

The solution of constitutive equations for viscoelastic fluids involves some important considerations, as for instance, the theoretical issues concerning the existence results [10, 16, 29, 46], and the development of numerical schemes for solving complex fluid flows [13, 20, 24].

Some forms of viscoelastic constitutive equations can be constructed considering the upper-convected time derivative or Oldroyd derivative [39], which is defined as

$$\overset{\nabla}{\zeta} := \frac{\partial \zeta}{\partial t} + (u \cdot \nabla) \zeta - (\nabla u) \zeta - \zeta (\nabla u)^\top, \quad (1)$$

where $u(x, t) \in \mathbb{R}^d$ is the velocity field of the flow and $\zeta(x, t) \in \mathbb{R}_{\text{sym}}^{d \times d}$ is a tensor to represent the non-Newtonian contribution for $d = (1, 2, 3)$. Roughly speaking, the derivative form of (1) is generally used for describing responses of viscoelastic fluids, as for instance, the deformation induced by the rate of strain. Therefore, the upper-convected time derivative (1) is employed to formulate the constitutive equations of the most popular models, as for instance the Oldroyd-B, Phan-Tien–Tanner (PTT), Giesekus, etc [34, 47].

In particular, we are interested in the numerical approximations for model equations based on the classical differential constitutive equation for the Oldroyd-B fluid in a dimensionless form:

$$\zeta + Wi \overset{\nabla}{\zeta} = 2(1 - \beta) D(u), \quad (2)$$

*Departamento de Matemática Aplicada e Estatística, Instituto de Ciências Matemáticas e de Computação - ICMC Universidade de São Paulo - Campus de São Carlos (deboramedeiros@usp.br).

[†]Faculty of Mathematics and Physics, Kanazawa University, Kanazawa 920-1192, Japan (notsu@se.kanazawa-u.ac.jp).

[‡]Departamento de Matemática e Computação, Faculdade de Ciências e Tecnologia Universidade Estadual Paulista Júlio de Mesquita Filho, Presidente Prudente 19060-900, SP, Brazil (cassio.oishi@unesp.br).

where $D(u) = [\nabla u + (\nabla u)^\top]/2$ is the strain-rate tensor, and the non-dimensional positive parameters Wi and β are respectively the Weissenberg number and the viscosity ratio ($\beta \in (0, 1)$).

The Weissenberg number [59] is a parameter related to the memory of the fluid, i.e., for a viscoelastic material, the Wi is a dimensionless number which can represent the relaxation time of the fluid. From a rheological point-of-view, the Weissenberg number can be interpreted as a number which can be used to measure the competition between elastic and viscous forces present in the concept of the viscoelasticity. A naive form to interpret the mathematical effect of this non-dimensional number is considering if $Wi = 0$ in Eq. (1.2), and in this case, the stress, represented here by ζ , is given by an explicit relation with the strain-rate tensor $D(u)$. Otherwise, for $Wi \neq 0$, the relation between the stress and the velocity gradient (rate-of-strain) can be modeled by a differential model, as for instance Eq. (1.2). Notice that increasing the value of the Weissenberg number in Eq. (1.2), the convected time derivative assumes a more significant effect in the equation, and therefore, the numerical treatment of this term needs to be improved in order to obtain a correct approximation of the solution. More details concerning the effect of the Weissenberg number on the partial differential equations whose describe viscoelastic fluid flows can be found in the works of Renardy [45, 47].

From a numerical point of view, in order to preserve the stability of the solutions, Eulerian frameworks for solving equation (2) need to apply a high-order spatial discretization for treating the convective terms in (1). Generally, the methods for dealing with convection-dominant terms of the upper-convected time derivative are based on the explicit and implicit upwind methodologies [2, 21, 50]. Considering explicit upwind strategies, many numerical approaches have been proposed in the literature for solving constitutive equations of viscoelastic models based on Eq. (2), e.g. the Eulerian schemes using Finite-Element (FE) [9, 19, 23, 49], Finite-Volume (FV) [1, 12, 41, 43], Finite-Difference (FD) [17, 33, 56], etc. It is worth to notice that the main drawback of the explicit upwind schemes is the severe time step limitations, and the application of implicit time integrators has been used for developing more robust frameworks [8, 50, 60], where a typical example is the so-called CFL condition. However, the construction of fully implicit upwind algorithms is complex resulting in general in high-cost computational schemes due to the solution of large systems. An additional drawback of implicit upwind schemes for solving convection-dominant problems is the excessive numerical diffusion.

In a different framework, Lagrangian methods combined with the method of characteristics [5, 6, 14, 37, 51] for solving viscoelastic fluid flows have been proposed by [3, 4, 15, 28, 30–32]. In these schemes, the Eulerian discretization of the convective term in (1), i.e., $(u \cdot \nabla)\zeta$, is avoided by using a Lagrangian discretization of the material derivative, i.e., $\partial\zeta/\partial t + (u \cdot \nabla)\zeta$, with the idea of the method of characteristics. The idea is to consider the trajectory of a fluid particle and discretize the material derivative along the trajectory. Since it is natural from a physical viewpoint and such Lagrangian schemes have advantages, e.g., the symmetry of resulting coefficient matrices of the system of linear equations in the implicit framework, no artificial parameters and no need of the so-called CFL condition, they are useful for flow problems appearing in the field of scientific computing.

A different approach for avoiding numerical instabilities and to obtain accurate solutions of Eq. (2) is mathematically rooted on the concept of the generalized Lie derivatives (GLD) [25–27] which modifies the definition of Eq. (1). In particular, this elegant methodology was firstly presented by Lee and Xu [25] (see also a similar idea proposed in [42]). In that pioneer work, the authors reformulated Eq. (2) using some mathematical properties to define generalized Riccati equations in terms of GLD. In summary, the upper-convected time derivative (1) was re-written using the concept of the transition matrix. This idea was adopted in the context of the finite element discretization in Lee et al. [27] to numerically solve the Poiseuille flow between two parallel plates around a cylinder while in [25] the authors presented theoretical results concerning the discretized version of the formulation proposed in [27].

In spite of the good stability properties observed in the numerical results and the sophisticated theoretical analysis of the works in [25, 27], to the best knowledge of the authors, the application of the GLD for solving equations in the form of (2) is limited for finite element discretization resulting in schemes of (mainly) first-order in time. In [25], two finite element schemes of second-order in time are presented based on the Crank–Nicolson or the Adams–Bashforth method along the trajectory of fluid particle. There are, however, no truncation error analysis of second-order in time and no numerical results yet, while numerical results by a GLD-based finite element scheme of first-order in time are given in [27]. Therefore, main contributions of this work can be summarized as follows:

i) the combination of the GLD strategy with the method of characteristics to develop temporal second-order finite difference schemes for treating the upper-convected time derivative (1), and ii) the application of simple stable algorithms avoiding the need to solve large systems as commonly occur for implicit upwind schemes.

In this paper, we present finite difference approximations of the upper-convected time derivative (1) based on GLD, and apply them to simple models. The approximations are of second-order in time, where the truncation error of second-order in time is proved in Theorem 1, and a practical form is given in Corollary 1. To the best knowledge of the authors, it is noted that the form, cf. (22), in the corollary is new and that there are no proofs of truncation error of second-order in time for time-discretized approximations using GLD-approach. Combining the approximation with the (bi)linear ($p = 1$) and (bi)quadratic ($p = 2$) Lagrange interpolations, we present full discretizations of the upper-convective time derivative of second-order in time and p -th order in space, i.e., $O(\Delta t^2 + h^p)$, which are proved in Theorem 2. We present two numerical schemes for simple models in d -dimensional spaces ($d = 1, 2$), cf. (32), which are both explicit. The difference of the schemes is the accuracy in space, i.e., one is of first-order ($p = 1$) and the other is of second-order ($p = 2$) in space as (bi)linear and (bi)quadratic Lagrange interpolation operators have been employed, respectively. After the presentation of the schemes, numerical experiments for simple models in d -dimensional spaces ($d = 1, 2$) are presented. They are consistent with the theoretical accuracies shown in Theorem 2.

In the case of Lagrangian finite element methods (often called Lagrange–Galerkin methods), a numerical integration is often employed in real computation for an integration of a composite function, since it is not easy to compute the integration of a composite function exactly. In fact, a rough numerical integration may cause instability, cf. [52, 53], where a robustness of a scheme of second-order in time with a choice of Δt depending on h is discussed in the papers. On the other hand, a quadrature-free scheme is proposed by using a mass-lumping technique in [44], and schemes with the exact integration of a composite function are proposed by introducing a linear interpolation of the velocity and implemented in two-dimensional numerical experiments in [54, 55]. In these quadrature-free schemes, there is no discrepancy between the theory and real computation. Besides them, to the best of our knowledge, it is still a standard technique for the integration of a composite function to employ a high-order quadrature rule, cf., e.g., [7, 11, 22, 36, 37], whose computation cost depends mainly on the number of quadrature points. In the end, we need to choose a suitable high-order quadrature rule by considering the computation cost and the *error* depending on the (expected) solution, Δt , h and so on. In the case of Lagrangian finite difference method, however, there is no need to choose a quadrature rule as no integration is used. This is an advantage of the Lagrangian finite difference method, cf [35]. The GLD-type Lagrangian finite difference schemes which will be presented in this paper also have this advantage.

The paper is organized as follows. In Section 2, basic concepts for the flow map and the upper-convected time derivative in the framework of the generalized Lie derivative and a simple model to be dealt in this paper are introduced. In Section 3, finite difference discretizations of the upper-convected time derivative are presented, where truncation errors are proved. In Section 4, GLD-type numerical schemes of second-order in time and p -th order in space for the simple model and their algorithms are presented. In Section 5, numerical results by our schemes are presented to see the experimental orders of convergence. In Section 6, conclusions are given. In Appendix, properties of GLD introduced in Section 2 are proved, and the main algorithms of the work are described in details.

2 Preliminaries

In this section, we present some basic concepts concerning the flow map and the ideas of the generalized Lie derivatives. For these purposes, we need to consider some mathematical statements.

Let $\Omega \subset \mathbb{R}^d$ ($d = 1, 2, 3$) be a bounded domain and T be a positive constant. Let $u : \Omega \times (0, T) \rightarrow \mathbb{R}^d$ be a given velocity with the following hypothesis:

Hypothesis 1. *The velocity u is sufficiently smooth and satisfies $u|_{\partial\Omega} = 0$.*

Let $\Delta t > 0$ be a time increment, $N_T := \lfloor T/\Delta t \rfloor$ the total number of time steps, and $t^n := n\Delta t$ ($n \in \mathbb{Z}$). For a

function f defined in $\Omega \times (0, T)$, let $f^n := f(\cdot, t^n)$ be the function at n -th time step. We define two mappings $X_1, \tilde{X}_1 : \Omega \times (0, T) \rightarrow \mathbb{R}^d$ by

$$X_1(x, t) := x - \Delta t u(x, t), \quad \tilde{X}_1(x, t) := x - 2\Delta t u(x, t),$$

which are upwind points of x with respect to $u(x, t)$. We introduce a symbol “ \circ ” to represent a composition of functions defined by

$$(g \circ X_1^n)(x) := g(X_1^n(x)),$$

for a function g defined in Ω , where $X_1^n(x) = X_1(x, t^n) = x - \Delta t u^n(x)$. We prepare a hypothesis for Δt :

Hypothesis 2. *The time increment Δt satisfies $\Delta t |u|_{C^0([0, T]; W^{1, \infty}(\Omega)^d)} \leq 1/8$.*

Remark 1. *Hypotheses 1 and 2 ensure that $X_1(\Omega, t) = \tilde{X}_1(\Omega, t) = \Omega$, and that Jacobians of the mappings $X_1(\cdot, t)$ and $\tilde{X}_1(\cdot, t)$ are greater than or equal to $1/2$, for $t \in [0, T]$, cf. [48, 55]. We note that Hypothesis 2 has no relation with the so-called CFL condition as any spatial mesh size is not included in it.*

2.1 Lagrangian framework and the generalized Lie derivative

For a fixed $(x, t) \in \bar{\Omega} \times [0, T]$, let $X(x, t; s) \in \mathbb{R}^d$ be a solution of the following ordinary differential equation with an initial condition:

$$\frac{\partial}{\partial s} X(x, t; s) = u(X(x, t; s), s), \quad s \in (0, T), \quad (3a)$$

$$X(x, t; t) = x, \quad (3b)$$

for $(x, t) \in \Omega \times (0, T)$. Physically, $X(x, t; s)$ gives the position of fluid particle at time s whose position at time t is x . It is known as a flow map and an illustration of this concept can be seen in Fig. 1.

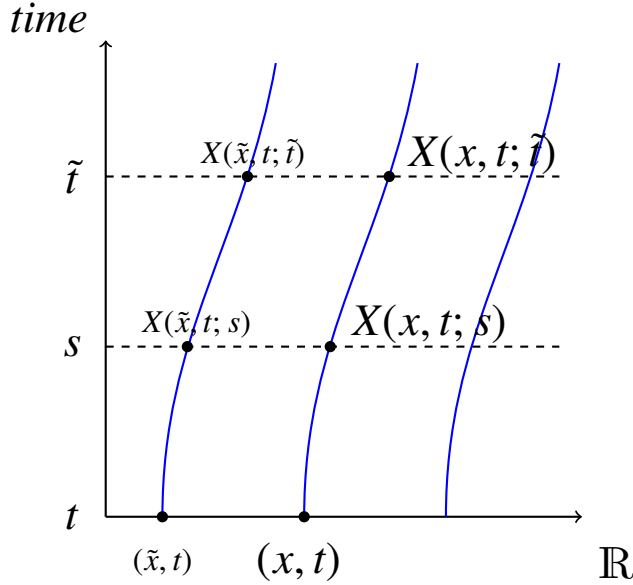


Fig. 1: Sketch of the flow map for $X(x, t; s)$.

For $(x, t) \in \Omega \times (0, T)$, let us introduce a matrix valued function $L(x, t; \cdot, \cdot) : (0, T) \times (0, T) \rightarrow \mathbb{R}^{d \times d}$ defined by

$$L_{ij}(x, t; t_1, t_2) := \left[\frac{\partial}{\partial z_j} X_i(z, t_1; t_2) \right]_{z=X(x, t; t_1)}, \quad i, j = 1, \dots, d, \quad (4)$$

which is the so-called deformation gradient. It is known that the function L has the following properties:

$$L(x, t; t_1, t_2)L(x, t; t_2, t_1) = L(x, t; t_1, t_1) = I, \quad (5a)$$

$$\frac{\partial}{\partial s}L(x, t; t_1, s) = (\nabla u)(X(x, t; s), s)L(x, t; t_1, s), \quad (5b)$$

$$\frac{\partial}{\partial s}L(x, t; s, t_1) = -L(x, t; s, t_1)(\nabla u)(X(x, t; s), s), \quad (5c)$$

for $t_1, t_2 \in [0, T]$, where $I \in \mathbb{R}_{\text{sym}}^{d \times d}$ is the identity matrix. Although the proofs can be found in, e.g., [27], we give the proofs again in Appendix A.1 under the assumption of unique existence of smooth regular L .

Let D/Dt be the material derivation defined by

$$\frac{D}{Dt} := \frac{\partial}{\partial t} + u \cdot \nabla.$$

For a function $\zeta : \Omega \times (0, T) \rightarrow \mathbb{R}^{d \times d}$, it is well-known that the material derivative of ζ can be written as

$$\frac{D\zeta}{Dt}(x, t) = \left[\frac{\partial \zeta}{\partial t} + (u \cdot \nabla)\zeta \right](x, t) = \frac{\partial}{\partial s}\zeta(X(x, t; s), s)|_{s=t}. \quad (6)$$

Here, we define the so-called generalized Lie derivative $\mathcal{L}_u\zeta$ by

$$(\mathcal{L}_u\zeta)(X(x, t; s), s) := L(x, t; t, s)\frac{\partial}{\partial s}\left[L(x, t; s, t)\zeta(X(x, t; s), s)L(x, t; s, t)^\top\right]L(x, t; t, s)^\top. \quad (7)$$

From (5), the upper-convected time derivative can be rewritten by using $\mathcal{L}_u\zeta$, i.e.,

$$\overset{\vee}{\zeta}(x, t) = (\mathcal{L}_u\zeta)(x, t) = (\mathcal{L}_u\zeta)(X(x, t; s), s)|_{s=t}, \quad (8)$$

which is shown in Appendix A.2.

2.2 The model equation

Based on the above description, we consider a simplified model equation in order to present the application of finite difference schemes for dealing with the generalized Lie derivative. Particularly, based on the Oldroyd-B constitutive equation (2), the problem is to find $\zeta : \Omega \times (0, T) \rightarrow \mathbb{R}_{\text{sym}}^{d \times d}$ such that

$$\overset{\vee}{\zeta} = F \quad \text{in } \Omega \times (0, T), \quad (9a)$$

$$\zeta = \zeta_{\text{in}} \quad \text{on } \Gamma_{\text{in}} \times (0, T), \quad (9b)$$

$$\zeta = \zeta^0 \quad \text{in } \Omega, \text{ at } t = 0, \quad (9c)$$

where Γ_{in} is an inflow boundary defined by $\Gamma_{\text{in}} := \{x \in \partial\Omega; u(x, t) \cdot n(x) < 0\}$ for the outward unit normal vector $n : \partial\Omega \rightarrow \mathbb{R}^d$, and $F : \Omega \times (0, T) \rightarrow \mathbb{R}_{\text{sym}}^{d \times d}$, $\zeta_{\text{in}} : \Gamma_{\text{in}} \times (0, T) \rightarrow \mathbb{R}_{\text{sym}}^{d \times d}$ and $\zeta^0 : \Omega \rightarrow \mathbb{R}_{\text{sym}}^{d \times d}$ are given functions.

Remark 2. (i) From (8), Eq. (9a) can be reformulated using the generalized Lie derivative resulting in:

$$\mathcal{L}_u\zeta = F \quad \text{in } \Omega \times (0, T). \quad (10)$$

(ii) In general, the inflow boundary Γ_{in} depends on time t , i.e., $\Gamma_{\text{in}} = \Gamma_{\text{in}}(t)$, while Γ_{in} is the empty set under Hypothesis 1. Throughout the paper, we deal with the inflow boundary Γ_{in} independent of time $t \in (0, T)$.

3 Finite difference discretizations

In this section, we present descriptions concerning the spatial and temporal discretizations. The main results related to the numerical analysis of the schemes are also described in details.

3.1 Space discretizations and interpolation operators

In this subsection, we introduce spatial discretizations and interpolation operators in one- and two-dimensions. Before starting them, for an integer i and a positive number δ , we prepare two functions $\eta_i^{(1)}(\cdot; \delta)$ and $\eta_i^{(2)}(\cdot; \delta) : \mathbb{R} \rightarrow \mathbb{R}$. The former, $\eta_i^{(1)}(\cdot; \delta)$, is defined by

$$\eta_i^{(1)}(s; \delta) := \begin{cases} \frac{s}{\delta} - i + 1 & (s \in [(i-1)\delta, i\delta]), \\ i + 1 - \frac{s}{\delta} & (s \in [i\delta, (i+1)\delta]), \\ 0 & (\text{otherwise}), \end{cases}$$

and the latter, $\eta_i^{(2)}(\cdot; \delta)$, is defined by

(i) i : even number

$$\eta_i^{(2)}(s; \delta) := \begin{cases} \left(\frac{s}{\delta} - i + 1\right)\left(\frac{s}{2\delta} - \frac{i}{2} + 1\right) & (s \in [(i-2)\delta, i\delta]), \\ \left(i + 1 - \frac{s}{\delta}\right)\left(\frac{i}{2} + 1 - \frac{s}{2\delta}\right) & (s \in [i\delta, (i+2)\delta]), \\ 0 & (\text{otherwise}), \end{cases}$$

(ii) i : odd number

$$\eta_i^{(2)}(s; \delta) := \begin{cases} \left(\frac{s}{\delta} - i + 1\right)\left(i + 1 - \frac{s}{\delta}\right) & (s \in [(i-1)\delta, (i+1)\delta]), \\ 0 & (\text{otherwise}). \end{cases}$$

The functions $\eta_i^{(1)}(\cdot; \delta)$ and $\eta_i^{(2)}(\cdot; \delta)$ are used below for the definitions of (bi)linear and (bi)quadratic interpolation operators $\Pi_h^{(1)}$ and $\Pi_h^{(2)}$, respectively.

3.1.1 One-dimensional case ($d = 1$)

Initially, we consider one spatial dimension, i.e., $d = 1$. For the sake of simplicity, we assume $\Omega = (0, a)$ for a positive number a . Let $N \in \mathbb{N}$ be a number, $h := a/N$ a mesh size, and $x_i := ih$ ($i \in \mathbb{Z}$) lattice points. We define a set of lattice points $\bar{\Omega}_h$ and a discrete function space V_h restrict to the number N , by

$$\begin{aligned} \bar{\Omega}_h &:= \{x_i \in \bar{\Omega}; i = 0, \dots, N\} \subset \bar{\Omega} \subset \mathbb{R}^d = \mathbb{R}, \\ V_h &:= \{v_h : \bar{\Omega}_h \rightarrow \mathbb{R}_{\text{sym}}^{d \times d}\} = \{v_h : \bar{\Omega}_h \rightarrow \mathbb{R}\}. \end{aligned}$$

We introduce a set of basis functions $\{\varphi_i^{(1)} : \bar{\Omega} \rightarrow \mathbb{R}; i = 0, \dots, N\}$ defined by

$$\varphi_i^{(1)}(x) := \eta_i^{(1)}(x; h), \quad i = 0, \dots, N.$$

The functions $\varphi_0^{(1)}$ and $\varphi_N^{(1)}$ are simplified to

$$\begin{aligned} \varphi_0^{(1)}(x) &:= \begin{cases} 1 - \frac{x}{h} & (x \in [x_0, x_1]) \\ 0 & (\text{otherwise}) \end{cases} = \begin{cases} \frac{x_1 - x}{h} & (x \in [x_0, x_1]) \\ 0 & (\text{otherwise}) \end{cases}, \\ \varphi_N^{(1)}(x) &:= \begin{cases} \frac{x}{h} - N + 1 & (x \in [x_{N-1}, x_N]) \\ 0 & (\text{otherwise}) \end{cases} = \begin{cases} \frac{x - x_{N-1}}{h} & (x \in [x_{N-1}, x_N]) \\ 0 & (\text{otherwise}) \end{cases}, \end{aligned}$$

as defined in $\bar{\Omega} = [x_0, x_N] = [0, a]$. Let $\Pi_h^{(1)} : V_h \rightarrow C^0(\bar{\Omega})$ be the linear interpolation operator defined by

$$(\Pi_h^{(1)} v_h)(x) := \sum_{i=0}^N v_h(x_i) \varphi_i^{(1)}(x).$$

We describe the ideas for using a quadratic interpolation. Let $N \in \mathbb{N}$ be an even number, and $M := N/2 \in \mathbb{N}$. For the definition of the quadratic interpolation operator $\Pi_h^{(2)}$, we define a set of basis functions $\{\varphi_i^{(2)} : \bar{\Omega} \rightarrow \mathbb{R}; i = 0, \dots, N\}$ by

$$\varphi_i^{(2)}(x) := \eta_i^{(2)}(x; h), \quad i = 0, \dots, N,$$

where $\varphi_0^{(2)}$ and $\varphi_N^{(2)}$ ($= \varphi_{2M}^{(2)}$) are reduced to

$$\varphi_0^{(2)}(x) = \begin{cases} \frac{(x_1 - x)(x_2 - x)}{2h^2} & (x \in [x_0, x_2]), \\ 0 & (\text{otherwise}), \end{cases}$$

$$\varphi_N^{(2)}(x) = \begin{cases} \frac{(x - x_{N-1})(x - x_{N-2})}{2h^2} & (x \in [x_{N-2}, x_N]), \\ 0 & (\text{otherwise}). \end{cases}$$

Let $\Pi_h^{(2)} : V_h \rightarrow C^0(\bar{\Omega})$ be the quadratic interpolation operator defined by

$$(\Pi_h^{(2)} v_h)(x) := \sum_{i=0}^N v_h(x_i) \varphi_i^{(2)}(x).$$

Remark 3. For $\alpha, \beta \in \mathbb{R}$ ($\alpha < \beta$), and $N_0 \in \mathbb{N}$ with $\delta_0 = \delta_0(\alpha, \beta, N_0) := (\beta - \alpha)/N_0 > 0$, let $I(\cdot; \alpha, \beta, N_0) : \mathbb{R} \rightarrow \{0, \dots, N_0\}$ be an integer-valued index indicator function defined by

$$I(s; \alpha, \beta, N_0) := \begin{cases} \left\lfloor \frac{s - \alpha}{\delta_0} \right\rfloor & (s \in (\alpha, \beta)), \\ 0 & (s \leq \alpha), \\ N_0 & (s \geq \beta). \end{cases} \quad (11)$$

We note that the integer $i_0 = I(s; \alpha, \beta, N_0)$ satisfies $i_0 \delta_0 + \alpha \leq s < (i_0 + 1) \delta_0 + \alpha$ for $s \in (\alpha, \beta)$, and that, for an even number N_0 with $M_0 = N_0/2 \in \mathbb{N}$, the integer $k_0 = I(s; \alpha, \beta, M_0)$ satisfies $2k_0 \delta_0 + \alpha \leq s < 2(k_0 + 1) \delta_0 + \alpha$ for $s \in (\alpha, \beta)$ as $\delta_0 = (\beta - \alpha)/M_0 = 2(\beta - \alpha)/N_0$.

For $d = 1$, we introduce two notations of intervals,

$$K_{i+1/2}^{(1)} := [x_i, x_{i+1}], \quad i \in \{0, \dots, N-1\},$$

$$K_{2k+1}^{(2)} := [x_{2k}, x_{2k+2}], \quad k \in \{0, \dots, M-1\},$$

whose measures are h and $2h$, respectively. Let $x \in \mathbb{R}$ be given arbitrarily. Then, the following are practically useful in computation:

(i) Let $i_0 := I(x; 0, a, N) \in \{0, \dots, N\}$. When $x \in \Omega$, the integer i_0 satisfies $x \in K_{i_0+1/2}^{(1)} = [x_{i_0}, x_{i_0+1}]$, and we have two-points representation of $(\Pi_h^{(1)} v_h)(x)$,

$$(\Pi_h^{(1)} v_h)(x) = v_{i_0} \varphi_{i_0}^{(1)}(x) + v_{i_0+1} \varphi_{i_0+1}^{(1)}(x), \quad (12)$$

where we have used a notation $v_i = v_h(x_i)$.

(ii) Let $k_0 := I(x; 0, a, M) \in \{0, \dots, M\}$. When $x \in \Omega$, the integer k_0 satisfies $x \in K_{2k_0+1}^{(2)} = [x_{2k_0}, x_{2k_0+2}]$, and we have three-points representation of $(\Pi_h^{(2)} v_h)(x)$,

$$(\Pi_h^{(2)} v_h)(x) = v_{2k_0} \varphi_{2k_0}^{(2)}(x) + v_{2k_0+1} \varphi_{2k_0+1}^{(2)}(x) + v_{2k_0+2} \varphi_{2k_0+2}^{(2)}(x), \quad (13)$$

for $v_i = v_h(x_i)$.

(iii) If the value $(\Pi_h^{(p)} v_h)(x)$ ($p = 1, 2$) is needed for $x \notin \Omega$, we can employ, instead of it, the closest end value of v_h , i.e., $v_0 = v_h(0)$ ($x \leq 0$) or $v_N = v_h(a)$ ($x \geq a$), while the value v_0 or v_N should be given by using ζ_{in} as x corresponds to an upwind point and $x \notin \bar{\Omega}$ means the high possibility of existence of ‘‘inflow’’ boundary near x . The function $\mathcal{I}(\cdot; \alpha, \beta, N)$ is, therefore, also useful for $x \notin \Omega$ in the sense that $\mathcal{I}(x; \alpha, \beta, N)$ provides the closest index of lattice point.

3.1.2 Two-dimensional case ($d = 2$)

We consider two spatial dimensions, i.e., $d = 2$. For the sake of simplicity, we assume $\Omega = (0, a_1) \times (0, a_2)$ for positive numbers a_1 and a_2 . Let $N_i \in \mathbb{N}$ ($i = 1, 2$) be numbers, $h_i := a_i/N_i$ ($i = 1, 2$) mesh sizes in x_i -direction, $h_{\min} := \min\{h_i; i = 1, \dots, d\}$ and $h = h_{\max} := \max\{h_i; i = 1, \dots, d\}$ minimum and maximum mesh sizes, and $x_{i,j} := (ih_1, jh_2)^\top$ ($i, j \in \mathbb{Z}$) lattice points. We assume a family of meshes satisfying the next hypothesis:

Hypothesis 3. *There exist positive constants h_0, γ_1 and γ_2 such that*

$$h \in (0, h_0], \quad \text{and} \quad \gamma_1 \leq \frac{h}{h_{\min}} \leq \gamma_2.$$

Remark 4. *The hypothesis is set for $d = 2$ essentially, as it always holds for $d = 1$ with $\gamma_1 = \gamma_2 = 1$.*

We define a set of lattice points $\bar{\Omega}_h$ and a discrete function space V_h restrict to the numbers $N_i \in \mathbb{N}$ ($i = 1, 2$), by

$$\begin{aligned} \bar{\Omega}_h &:= \{x_{i,j} \in \bar{\Omega}; i = 0, \dots, N_1, j = 0, \dots, N_2\}, \\ V_h &:= \{v_h : \bar{\Omega}_h \rightarrow \mathbb{R}^{d \times d}_{\text{sym}}\}, \end{aligned}$$

where it is noted that $\bar{\Omega}_h \subset \bar{\Omega} \subset \mathbb{R}^d$ ($= \mathbb{R}^2$). Using $\eta_i^{(1)}(\cdot; \delta)$, we introduce a set of basis functions $\{\varphi_{i,j}^{(1)} : \bar{\Omega} \rightarrow \mathbb{R}; x_{i,j} \in \bar{\Omega}_h, i, j \in \mathbb{Z}\}$ defined by

$$\varphi_{i,j}^{(1)}(x) = \varphi_{i,j}^{(1)}(x_1, x_2) := \eta_i^{(1)}(x_1; h_1) \eta_j^{(1)}(x_2; h_2).$$

Let $\Pi_h^{(1)} : V_h \rightarrow C^0(\bar{\Omega})$ be the bilinear interpolation operator defined by

$$(\Pi_h^{(1)} v_h)(x) := \sum_{x_{i,j} \in \bar{\Omega}_h} v_h(x_{i,j}) \varphi_{i,j}^{(1)}(x).$$

The extension of the above interpolation using the biquadratic interpolation strategy can be defined as follows. Let $N_1, N_2 \in \mathbb{N}$ be even numbers, and $M_i := N_i/2 \in \mathbb{N}$ for $i = 1, 2$. For the definition of the biquadratic interpolation operator $\Pi_h^{(2)}$, we introduce basis functions $\{\varphi_{i,j}^{(2)} : \bar{\Omega} \rightarrow \mathbb{R}; x_{i,j} \in \bar{\Omega}_h\}$ defined by

$$\varphi_{i,j}^{(2)}(x) = \varphi_{i,j}^{(2)}(x_1, x_2) := \eta_i^{(2)}(x_1; h_1) \eta_j^{(2)}(x_2; h_2).$$

Let $\Pi_h^{(2)} : V_h \rightarrow C^0(\bar{\Omega})$ be the biquadratic interpolation operator defined by

$$(\Pi_h^{(2)} v_h)(x) := \sum_{x_{i,j} \in \bar{\Omega}_h} v_h(x_{i,j}) \varphi_{i,j}^{(2)}(x).$$

Remark 5. *For $d = 2$, we introduce two notations of boxes (cells),*

$$\begin{aligned} K_{i+1/2, j+1/2}^{(1)} &:= [ih_1, (i+1)h_1] \times [jh_2, (j+1)h_2], & (i, j) &\in \{0, \dots, N_1 - 1\} \times \{0, \dots, N_2 - 1\}, \\ K_{2k+1, 2l+1}^{(2)} &:= [2kh_1, (2k+2)h_1] \times [2lh_2, (2l+2)h_2], & (k, l) &\in \{0, \dots, M_1 - 1\} \times \{0, \dots, M_2 - 1\}, \end{aligned}$$

whose measures are $h_1 h_2$ and $4h_1 h_2$, respectively. Let $x \in \mathbb{R}^2$ be given arbitrarily. Then, the following are practically useful in computation:

(i) Let $i_0 := \mathcal{I}(x_1; 0, a_1, N_1) \in \{0, \dots, N_1\}$ and $j_0 := \mathcal{I}(x_2; 0, a_2, N_2) \in \{0, \dots, N_2\}$. When $x \in \Omega$, the set of integers (i_0, j_0) satisfies $x \in K_{i_0+1/2, j_0+1/2}^{(1)} = [i_0 h_1, (i_0 + 1)h_1] \times [j_0 h_2, (j_0 + 1)h_2]$, and we have four-points representation of $(\Pi_h^{(1)} v_h)(x)$,

$$(\Pi_h^{(1)} v_h)(x) = \sum_{m,n=0,1} v_{i_0+m, j_0+n} \varphi_{i_0+m, j_0+n}^{(1)}(x), \quad (14)$$

where we have used a simplified notation $v_{i,j} = v_h(x_{i,j})$.

(ii) Let $k_0 := \mathcal{I}(x_1; 0, a_1, M_1) \in \{0, \dots, M_1\}$ and $l_0 := \mathcal{I}(x_2; 0, a_2, M_2) \in \{0, \dots, M_2\}$. When $x \in \Omega$, the integer k_0 satisfies $x \in K_{2k_0+1}^{(2)} = [x_{2k_0}, x_{2k_0+2}]$, and we have nine-points representation of $(\Pi_h^{(2)} v_h)(x)$,

$$(\Pi_h^{(2)} v_h)(x) = \sum_{m,n=0,1,2} v_{2k_0+m, 2l_0+n} \varphi_{2k_0+m, 2l_0+n}^{(2)}(x). \quad (15)$$

(iii) If the value $(\Pi_h^{(p)} v_h)(x)$ ($p = 1, 2$) is needed for $x \notin \Omega$, we can employ, instead of it, the closest end value of v_h , i.e., one of the values of $v_h(x_{i,j})$ ($x_{i,j} \in \bar{\Omega}_h \cap \partial\Omega$), while the value should be given by using ζ_{in} as x corresponds to an upwind point.

Remark 6. We omit the extension of the interpolation operators $\Pi_h^{(p)}$ ($p = 1, 2$) to the three-dimensional case, i.e., $d = 3$, since it is naturally defined by introducing basis functions $\varphi_{i,j,k}^{(p)}(x) = \varphi_{i,j,k}^{(p)}(x_1, x_2, x_3) := \eta_i^{(p)}(x_1; h_1) \eta_j^{(p)}(x_2; h_2) \eta_k^{(p)}(x_3; h_3)$ for $p = 1, 2$ in a similar manner.

3.2 Time discretization: truncation error analysis

For the velocity u , let $L_1, \tilde{L}_1 : \Omega \times (0, T) \rightarrow \mathbb{R}^{d \times d}$ be matrices defined by

$$L_1(x, t) := I + \Delta t(\nabla u)(x, t), \quad \tilde{L}_1(x, t) := I + 2\Delta t(\nabla u)(x, t), \quad (16)$$

which are approximations of $L(x, t; t - \Delta t, t)$ and $L(x, t; t - 2\Delta t, t)$, respectively, cf. Lemma 1 below. Now, we present a theorem which provides an approximation of the upper-convected time derivative of second-order in time.

Theorem 1. Suppose that Hypotheses 1 and 2 hold true. Let $\zeta : \bar{\Omega} \times [0, T] \rightarrow \mathbb{R}^{d \times d}$ be a sufficiently smooth function. Then, for any $x \in \bar{\Omega}$ and $t \in [2\Delta t, T]$, we have

$$\begin{aligned} \overset{\vee}{\zeta}(x, t) &= \frac{1}{2\Delta t} \left[3\zeta(x, t) - 4L_1(x, t)\zeta(X_1(x, t), t - \Delta t)L_1(x, t)^\top \right. \\ &\quad \left. + \tilde{L}_1(x, t)\zeta(\tilde{X}_1(x, t), t - 2\Delta t)\tilde{L}_1(x, t)^\top \right] + O(\Delta t^2). \end{aligned} \quad (17)$$

We give the proof of Theorem 1 after giving a remark and preparing two lemmas.

Remark 7. (i) Let us consider $(x, t) \in \bar{\Omega} \times [2\Delta t, T]$ as a fixed point and employ simple notations $X = X(x, t; \cdot)$ and $L(\cdot, \cdot) = L(x, t; \cdot, \cdot)$. Then, an approximation of $\overset{\vee}{\zeta}(x, t)$ of first-order in time is obtained as follows:

$$\begin{aligned} \overset{\vee}{\zeta}(x, t) &= (\mathcal{L}_u \zeta)(X(s), s) \Big|_{s=t} && \text{(by (8))} \\ &= L(t, s) \frac{\partial}{\partial s} \left[L(s, t) \zeta(X(s), s) L(s, t)^\top \right] L(t, s)^\top \Big|_{s=t} && \text{(by definition (7))} \\ &= L(t, s) \frac{1}{\Delta t} \left[L(s, t) \zeta(X(s), s) L(s, t)^\top \right. \\ &\quad \left. - L(s - \Delta t, t) \zeta(X(s - \Delta t), s - \Delta t) L(s - \Delta t, t)^\top \right] L(t, s)^\top \Big|_{s=t} + O(\Delta t) \end{aligned}$$

(by the Euler method with respect to s)

$$\begin{aligned}
&= \frac{1}{\Delta t} \left[\zeta(X(t), t) - L(t - \Delta t, t) \zeta(X(t - \Delta t), t - \Delta t) L(t - \Delta t, t)^\top \right] + O(\Delta t) \\
&\quad \text{(by substituting } t \text{ into } s \text{ and (5a))} \\
&= \frac{1}{\Delta t} \left[\zeta(x, t) - L_1(x, t) \zeta(X_1(x, t), t - \Delta t) L_1(x, t)^\top \right] + O(\Delta t),
\end{aligned}$$

where the last equality holds true from the initial condition (3b) for X , i.e., $X(t) = x$, and the relations,

$$L_1(x, t) = L(t - \Delta t, t) + O(\Delta t^2), \quad X_1(x, t) = X(t - \Delta t) + O(\Delta t^2),$$

which will be shown in Lemmas 1 and 2 with $k = 1$ below, respectively.

(ii) Theorem 1 presents an approximation of $\check{\zeta}(x, t)$ of second-order in time based on the two-step Adams–Bashforth method, i.e., for a smooth function $f : \mathbb{R} \rightarrow \mathbb{R}$,

$$f'(t) = \frac{d}{ds} f(s) \Big|_{s=t} = \frac{1}{2\Delta t} [3f(t) - 4f(t - \Delta t) + f(t - 2\Delta t)] + O(\Delta t^2),$$

in place of the Euler method in (i).

Lemma 1. Suppose that Hypotheses 1 and 2 hold true. Let $k = 1$ or 2 be fixed. Then, for any $x \in \bar{\Omega}$ and $t \in [k\Delta t, T]$, we have

$$L(x, t; t - k\Delta t, t) = I + k\Delta t(\nabla u)(x, t) + \frac{(k\Delta t)^2}{2} U(x, t) + O(\Delta t^3), \quad (18)$$

where $U : \Omega \times (0, T) \rightarrow \mathbb{R}^{d \times d}$ is a function defined by

$$U := (\nabla u)^2 - \frac{D(\nabla u)}{Dt}.$$

Proof. From the Taylor expansion, we have

$$\begin{aligned}
L(x, t; t - k\Delta t, t) &= L(x, t; s - k\Delta t, t) \Big|_{s=t} \\
&= \left[L(x, t; s, t) - k\Delta t \frac{\partial}{\partial s} L(x, t; s, t) + \frac{(k\Delta t)^2}{2} \frac{\partial^2}{\partial s^2} L(x, t; s, t) \right] \Big|_{s=t} + O(\Delta t^3) \\
&= \left[L(x, t; s, t) - k\Delta t [-L(x, t; s, t)(\nabla u)(X(x, t; s), s)] + \right. \\
&\quad \left. + \frac{(k\Delta t)^2}{2} \frac{\partial}{\partial s} [-L(x, t; s, t)(\nabla u)(X(x, t; s), s)] \right] \Big|_{s=t} + O(\Delta t^3) \quad \text{(by (5c))} \\
&= I + k\Delta t(\nabla u)(x, t) - \frac{(k\Delta t)^2}{2} \frac{\partial}{\partial s} [L(x, t; s, t)(\nabla u)(X(x, t; s), s)] \Big|_{s=t} + O(\Delta t^3). \quad (19)
\end{aligned}$$

We evaluate $\frac{\partial}{\partial s} [L(x, t; s, t)(\nabla u)(X(x, t; s), s)] \Big|_{s=t}$ as follows:

$$\begin{aligned}
&\frac{\partial}{\partial s} [L(x, t; s, t)(\nabla u)(X(x, t; s), s)] \Big|_{s=t} \\
&= \left[\left(\frac{\partial}{\partial s} L(x, t; s, t) \right) (\nabla u)(X(x, t; s), s) + L(x, t; s, t) \left(\frac{\partial}{\partial s} (\nabla u)(X(x, t; s), s) \right) \right] \Big|_{s=t} \\
&= \left[-L(x, t; s, t)(\nabla u)^2(X(x, t; s), s) + L(x, t; s, t) \frac{D(\nabla u)}{Dt}(X(x, t; s), s) \right] \Big|_{s=t} \\
&= -(\nabla u)^2(x, t) + \frac{D(\nabla u)}{Dt}(x, t) = -U(x, t). \quad (20)
\end{aligned}$$

Combining (20) with (19), we obtain (18). \square

Lemma 2. Suppose that Hypotheses 1 and 2 hold true. Let $k = 1$ or 2 be fixed. Then, for any $x \in \bar{\Omega}$ and $t \in [k\Delta t, T]$, we have the following:

(i) It holds that

$$X(x, t; t - k\Delta t) = x - k\Delta t u(x, t) + \frac{(k\Delta t)^2}{2} \frac{Du}{Dt}(x, t) + O(\Delta t^3).$$

(ii) Let $\zeta : \Omega \times (0, T) \rightarrow \mathbb{R}^{d \times d}$ be a sufficiently smooth function. It holds that

$$\zeta(X(x, t; t - k\Delta t), t - k\Delta t) = \zeta(x - k\Delta t u(x, t), t - k\Delta t) + \frac{(k\Delta t)^2}{2} Z(x, t) + O(\Delta t^3),$$

where $Z : \Omega \times (0, T) \rightarrow \mathbb{R}^{d \times d}$ is a function defined by

$$Z := \left(\frac{Du}{Dt} \cdot \nabla \right) \zeta.$$

Proof. We prove (i). Recalling that $X(x, t; s)$ is a solution to (3) and noting that the following identity,

$$X(x, t; t - k\Delta t) = x - \int_{t-k\Delta t}^t u(X(x, t; s), s) ds,$$

holds true, we have

$$\begin{aligned} & X(x, t; t - k\Delta t) - [x - k\Delta t u(x, t)] \\ &= x - \int_{t-k\Delta t}^t u(X(x, t; s), s) ds - \left[x - \int_{t-k\Delta t}^t u(X(x, t; t), t) ds \right] \\ &= \int_{t-k\Delta t}^t [u(X(x, t; t), t) - u(X(x, t; s), s)] ds = \int_{t-k\Delta t}^t ds [u(X(x, t; s_1), s_1)]_{s_1=s}^t \\ &= \int_{t-k\Delta t}^t ds \int_s^t \frac{Du}{Dt}(X(x, t; s_1), s_1) ds_1 = \int_{t-k\Delta t}^t ds \int_s^t \left(\frac{Du}{Dt}(x, t) + O(\Delta t) \right) ds_1 \\ &= \frac{(k\Delta t)^2}{2} \frac{Du}{Dt}(x, t) + O(\Delta t^3), \end{aligned}$$

which completes the proof of (i).

We prove (ii). From (i) and the Taylor expansion, we have

$$\begin{aligned} & \zeta(X(x, t; t - k\Delta t), t - k\Delta t) \\ &= \zeta\left(x - k\Delta t u(x, t) + \frac{(k\Delta t)^2}{2} \frac{Du}{Dt}(x, t), t - k\Delta t\right) + O(\Delta t^3) \\ &= \zeta(x - k\Delta t u(x, t), t - k\Delta t) + \frac{(k\Delta t)^2}{2} \left[\left(\frac{Du}{Dt}(x, t) \cdot \nabla \right) \zeta \right] (x - k\Delta t u(x, t), t - k\Delta t) + O(\Delta t^3) \\ &= \zeta(x - k\Delta t u(x, t), t - k\Delta t) + \frac{(k\Delta t)^2}{2} Z(x, t) + O(\Delta t^3), \end{aligned}$$

where we have used the relation,

$$\left[\left(\frac{Du}{Dt}(x, t) \cdot \nabla \right) \zeta \right] (x - k\Delta t u(x, t), t - k\Delta t) = Z(x, t) + O(\Delta t),$$

for the last equality. □

Proof of Theorem 1. In the proof, we often employ simple notations, $L(\cdot, \cdot) = L(x, t; \cdot, \cdot)$ and $X = X(x, t; \cdot)$, if there is no confusion, since (x, t) is considered as a fixed position in space and time. From the Adams–Bashforth method, i.e., for a smooth function g defined in \mathbb{R} , $g'(s) = \frac{1}{2\Delta t} [3g(s) - 4g(s - \Delta t) + g(s - 2\Delta t)] + O(\Delta t^2)$, we have

$$\overset{\vee}{\zeta}(x, t) = (\mathcal{L}_u \zeta)(x, t) = (\mathcal{L}_u \zeta)(X(s), s)_{|s=t} = L(t, s) \frac{\partial}{\partial s} \left[L(s, t) \zeta(X(s), s) L(s, t)^\top \right] L(t, s)^\top \Big|_{s=t}$$

$$\begin{aligned}
&= L(t, s) \frac{1}{2\Delta t} \left[3L(s, t) \zeta(X(s), s) L(s, t)^\top - 4L(s - \Delta t, t) \zeta(X(s - \Delta t), s - \Delta t) L(s - \Delta t, t)^\top \right. \\
&\quad \left. + L(s - 2\Delta t, t) \zeta(X(s - 2\Delta t), s - 2\Delta t) L(s - 2\Delta t, t)^\top \right] L(t, s)^\top \Big|_{s=t} + O(\Delta t^2) \\
&= \frac{1}{2\Delta t} \left[3\zeta(X(x, t; s), s) - 4L(t, s) L(s - \Delta t, t) \zeta(X(s - \Delta t), s - \Delta t) L(s - \Delta t, t)^\top L(t, s)^\top \right. \\
&\quad \left. + L(t, s) L(s - 2\Delta t, t) \zeta(X(s - 2\Delta t), s - 2\Delta t) L(s - 2\Delta t, t)^\top L(t, s)^\top \right] \Big|_{s=t} + O(\Delta t^2) \quad (\text{by (5a)}) \\
&= \frac{1}{2\Delta t} \left[3\zeta(x, t) - 4L(t - \Delta t, t) \zeta(X(t - \Delta t), t - \Delta t) L(t - \Delta t, t)^\top \right. \\
&\quad \left. + L(t - 2\Delta t, t) \zeta(X(t - 2\Delta t), t - 2\Delta t) L(t - 2\Delta t, t)^\top \right] + O(\Delta t^2) \quad (\text{by (3b) and (5a)}) \\
&= \frac{1}{2\Delta t} \left[3\zeta(x, t) - 4 \left[L_1 + \frac{\Delta t^2}{2} U \right] (x, t) \zeta(X(t - \Delta t), t - \Delta t) \left[L_1 + \frac{\Delta t^2}{2} U \right]^\top (x, t) \right. \\
&\quad \left. + \left[\tilde{L}_1 + 2\Delta t^2 U \right] (x, t) \zeta(X(t - 2\Delta t), t - 2\Delta t) \left[\tilde{L}_1 + 2\Delta t^2 U \right]^\top (x, t) \right] + O(\Delta t^2) \\
&\hspace{15em} (\text{by Lem. 1 with definitions of } L_1 \text{ and } \tilde{L}_1) \\
&= \frac{1}{2\Delta t} \left[3\zeta(x, t) - 4L_1(x, t) \zeta(X(t - \Delta t), t - \Delta t) L_1^\top(x, t) \right. \\
&\quad + \tilde{L}_1(x, t) \zeta(X(t - 2\Delta t), t - 2\Delta t) \tilde{L}_1^\top(x, t) \\
&\quad - 2\Delta t^2 [\zeta(X(t - \Delta t), t - \Delta t) - \zeta(X(t - 2\Delta t), t - 2\Delta t)] U^\top(x, t) \\
&\quad \left. - 2\Delta t^2 U(x, t) [\zeta(X(t - \Delta t), t - \Delta t) - \zeta(X(t - 2\Delta t), t - 2\Delta t)] \right] + O(\Delta t^2) \\
&= \frac{1}{2\Delta t} \left[3\zeta(x, t) - 4L_1(x, t) \zeta(X(t - \Delta t), t - \Delta t) L_1^\top(x, t) \right. \\
&\quad \left. + \tilde{L}_1(x, t) \zeta(X(t - 2\Delta t), t - 2\Delta t) \tilde{L}_1^\top(x, t) \right] + O(\Delta t^2), \tag{21}
\end{aligned}$$

where the relation,

$$\zeta(X(t - \Delta t), t - \Delta t) - \zeta(X(t - 2\Delta t), t - 2\Delta t) = O(\Delta t),$$

has been employed for the last equality. Combining Lemma 2-(ii) with (21) and recalling $x - \Delta t u(x, t) = X_1(x, t)$ and $x - 2\Delta t u(x, t) = \tilde{X}_1(x, t)$, we obtain

$$\begin{aligned}
\overset{\vee}{\zeta}(x, t) &= \frac{1}{2\Delta t} \left[3\zeta(x, t) - 4L_1(x, t) \zeta(X_1(x, t), t - \Delta t) L_1^\top(x, t) \right. \\
&\quad \left. + \tilde{L}_1(x, t) \zeta(\tilde{X}_1(x, t), t - 2\Delta t) \tilde{L}_1^\top(x, t) \right] + O(\Delta t^2),
\end{aligned}$$

which completes the proof. \square

Substituting t^n into t in (17), the discrete form of second-order in time for the upper-convected time derivative is given as follows.

Corollary 1. *Under the same assumptions of Theorem 1, we have*

$$\overset{\vee}{\zeta}(x, t^n) = \frac{1}{2\Delta t} \left[3\zeta^n(x) - 4L_1^n(x) (\zeta^{n-1} \circ X_1^n)(x) L_1^n(x)^\top + \tilde{L}_1^n(x) (\zeta^{n-2} \circ \tilde{X}_1^n)(x) \tilde{L}_1^n(x)^\top \right] + O(\Delta t^2) \tag{22}$$

for $n = 2, \dots, N_T$.

Remark 8. *Although the approximation (22) of $\overset{\vee}{\zeta}(x, t^n)$ of second-order in time is combined with the finite difference method in this paper below, one can combine it with other methods, e.g., the finite element method and the finite volume method.*

3.3 Full discretizations of the upper-convected time derivative

Suppose that $\zeta \in C([0, T]; C(\bar{\mathcal{Q}}; \mathbb{R}_{\text{sym}}^{d \times d}))$ and $\zeta_h = \{\zeta_h^n\}_{n=0}^{N_T} \subset V_h$ are given. For $n \in \{1, \dots, N_T\}$ and $p \in \{1, 2\}$, let $\mathcal{A}^n \zeta : \bar{\mathcal{Q}} \rightarrow \mathbb{R}_{\text{sym}}^{d \times d}$ and $\mathcal{A}_h^{n,(p)} \zeta_h : \bar{\mathcal{Q}}_h \rightarrow \mathbb{R}_{\text{sym}}^{d \times d}$ be functions defined by

$$\begin{aligned} [\mathcal{A}^n \zeta](x) &:= \begin{cases} \frac{1}{2\Delta t} \left[3\zeta^n(x) - 4L_1^n(x)(\zeta^{n-1} \circ X_1^n)(x)L_1^n(x)^\top \right. \\ \quad \left. + \tilde{L}_1^n(x)(\zeta^{n-2} \circ \tilde{X}_1^n)(x)\tilde{L}_1^n(x)^\top \right] & (n \geq 2), \\ \frac{1}{\Delta t} \left[\zeta^1(x) - L_1^1(x)(\zeta^0 \circ X_1^1)(x)L_1^1(x)^\top \right] & (n = 1), \end{cases} \\ [\mathcal{A}_h^{n,(p)} \zeta_h](x) &:= \begin{cases} \frac{1}{2\Delta t} \left[3\zeta_h^n(x) - 4L_1^n(x)[(I_h^{(p)} \zeta_h^{n-1}) \circ X_1^n](x)L_1^n(x)^\top \right. \\ \quad \left. + \tilde{L}_1^n(x)[(I_h^{(p)} \zeta_h^{n-2}) \circ \tilde{X}_1^n](x)\tilde{L}_1^n(x)^\top \right] & (n \geq 2), \\ \frac{1}{\Delta t} \left[\zeta_h^1(x) - L_1^1(x)[(I_h^{(p)} \zeta_h^0) \circ X_1^1](x)L_1^1(x)^\top \right] & (n = 1), \end{cases} \end{aligned} \quad (23)$$

respectively. Using the notation $\mathcal{A}^n \zeta$, we can write Eq. (22) as, for $n = \{2, \dots, N_T\}$,

$$\overset{\vee}{\zeta}(x, t^n) = [\mathcal{A}^n \zeta](x) + O(\Delta t^2).$$

Now, we present a theorem on the truncation error of our finite difference approximations of the upper-convected time derivative, where the function $\mathcal{A}_h^{n,(p)} \zeta : \bar{\mathcal{Q}}_h \rightarrow \mathbb{R}_{\text{sym}}^{d \times d}$ to be used in the theorem has meaning since $\zeta \in C([0, T]; C(\bar{\mathcal{Q}}; \mathbb{R}_{\text{sym}}^{d \times d}))$ can be considered as a series of functions in V_h , i.e., $\zeta = \{\zeta^n\}_{n=0}^{N_T} \subset V_h$.

Theorem 2. *Suppose that Hypotheses 1, 2 and 3 hold true. Let $\zeta : \bar{\mathcal{Q}} \times [0, T] \rightarrow \mathbb{R}^{d \times d}$ be a sufficiently smooth function. Then, we have*

$$\overset{\vee}{\zeta}(x, t^n) = [\mathcal{A}_h^{n,(p)} \zeta](x) + O(\Delta t^2 + h^p) \quad (24)$$

for $x \in \bar{\mathcal{Q}}_h$, $n \in \{2, \dots, N_T\}$ and $p = 1, 2$.

Proof. Since for $x \in \bar{\mathcal{Q}}_h$ we have

$$\begin{aligned} \overset{\vee}{\zeta}(x, t^n) &= [\mathcal{A}^n \zeta](x) + O(\Delta t^2) \\ &= [\mathcal{A}_h^{n,(p)} \zeta](x) - \left([\mathcal{A}_h^{n,(p)} \zeta](x) - [\mathcal{A}^n \zeta](x) \right) + O(\Delta t^2) \\ &= [\mathcal{A}_h^{n,(p)} \zeta](x) + \frac{2}{\Delta t} L_1^n(x) [(I_h^{(p)} \zeta^{n-1} - \zeta^{n-1}) \circ X_1^n](x) L_1^n(x)^\top \\ &\quad - \frac{1}{2\Delta t} \tilde{L}_1^n(x) [(I_h^{(p)} \zeta^{n-2} - \zeta^{n-2}) \circ \tilde{X}_1^n](x) \tilde{L}_1^n(x)^\top + O(\Delta t^2) \end{aligned} \quad (25)$$

from Corollary 1, it is enough for the proof to show the following estimates,

$$\frac{2}{\Delta t} [(I_h^{(p)} \zeta^{n-1} - \zeta^{n-1}) \circ X_1^n](x) = O(h^p), \quad (26a)$$

$$\frac{1}{2\Delta t} [(I_h^{(p)} \zeta^{n-2} - \zeta^{n-2}) \circ \tilde{X}_1^n](x) = O(h^p), \quad (26b)$$

where simple estimates (31) are easily obtained as shown in Remark 9 later and the key issue is to eliminate the negative order in Δt from (31) and get (26). We prove the former equality of (26) for $d = 2$ only, as the equality for $d = 1$ is simpler and the latter one is proved similarly. Let $x = x_{i,j} \in \bar{\mathcal{Q}}_h$ and $y^n := X_1^n(x) = x - u^n(x)\Delta t$. To simplify notations, we omit superscripts $n-1$ and n from ζ^{n-1} and y^n in the rest of proof, respectively, if there is no confusion.

Let us start with $p = 1$. From Hypotheses 1 and 2, we have $y \in \bar{\mathcal{Q}}$ and there exists a pair of indexes (i_0, j_0) such that $y \in K_{i_0+1/2, j_0+1/2}^{(1)} (= [i_0 h_1, (i_0 + 1)h_1] \times [j_0 h_2, (j_0 + 1)h_2])$. Let $\Lambda^{(1)}(y)$ be a set of pairs of indexes of lattice points near y defined by $\Lambda^{(1)}(y) := \{(i_0, j_0), (i_0 + 1, j_0), (i_0, j_0 + 1), (i_0 + 1, j_0 + 1)\}$. Let $a = (a_1, a_2)^\top := y - x_{i_0, j_0} = ((i - i_0)h_1 - u_1^n(x_{i,j})\Delta t, (j - j_0)h_2 - u_2^n(x_{i,j})\Delta t)$ and $\tilde{a} = (\tilde{a}_1, \tilde{a}_2)^\top := x_{i_0+1, j_0+1} - y$. Without loss of generality, we can assume that $u_k^n(x_{i,j}) \geq 0$ ($k = 1, 2$), $i_0 < i$, $j_0 < j$ and $a_k, \tilde{a}_k \geq 0$ ($k = 1, 2$), cf. Fig. 2. Then, we have

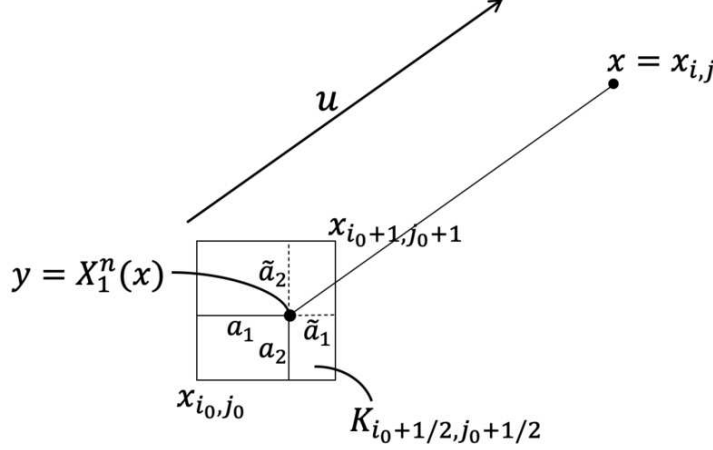


Fig. 2: Notations in the proof of Theorem 2

$$\begin{aligned}
& [(\Pi_h^{(1)} \zeta - \zeta) \circ X_1^n](x) = (\Pi_h^{(1)} \zeta)(y) - \zeta(y) \\
& = \sum_{(k,l) \in \Lambda^{(1)}(y)} [\zeta(x_{k,l}) - \zeta(y)] \varphi_{k,l}^{(1)}(y) \quad (\text{by } \sum_{(k,l) \in \Lambda^{(1)}(y)} \varphi_{k,l}^{(1)}(y) = 1) \\
& = \sum_{(k,l) \in \Lambda^{(1)}(y)} [\zeta(y + s(x_{k,l} - y))]_{s=0}^1 \varphi_{k,l}^{(1)}(y) \\
& = \sum_{(k,l) \in \Lambda^{(1)}(y)} \int_0^1 ([(x_{k,l} - y) \cdot \nabla] \zeta)(y + s_1(x_{k,l} - y)) ds_1 \varphi_{k,l}^{(1)}(y) \\
& = \sum_{(k,l) \in \Lambda^{(1)}(y)} \int_0^1 ds_1 \int_0^{s_1} ([(x_{k,l} - y) \cdot \nabla]^2 \zeta)(y + s_2(x_{k,l} - y)) ds_2 \varphi_{k,l}^{(1)}(y) \\
& \quad (\text{by } \sum_{(k,l) \in \Lambda^{(1)}(y)} ([(x_{k,l} - y) \cdot \nabla] \zeta)(y) \varphi_{k,l}^{(1)}(y) = 0),
\end{aligned} \tag{27}$$

and, for $(k, l) = (i_0, j_0)$,

$$\begin{aligned}
& \left| \int_0^1 ds_1 \int_0^{s_1} ([(x_{k,l} - y) \cdot \nabla]^2 \zeta)(y + s_2(x_{k,l} - y)) ds_2 \varphi_{k,l}^{(1)}(y) \right| = \left| \int_0^1 ds_1 \int_0^{s_1} ([a \cdot \nabla]^2 \zeta)(y - s_2 a) ds_2 \frac{\tilde{a}_1 \tilde{a}_2}{h_1 h_2} \right| \\
& \leq c_1 (a_1 + a_2)^2 \|\zeta^{n-1}\|_{C^2(K_{i_0+1/2, j_0+1/2}^{(1)}; \mathbb{R}^{d \times d}; \mathbb{R}^{\text{sym}})} \frac{\tilde{a}_1 \tilde{a}_2}{h_1 h_2} \leq c'_1 (a_1 \tilde{a}_1 + a_2 \tilde{a}_2) \|\zeta^{n-1}\|_{C^2(\bar{\mathcal{Q}}; \mathbb{R}^{d \times d}; \mathbb{R}^{\text{sym}})} \\
& \quad (\text{by } a_k, \tilde{a}_k \leq h_k, k = 1, 2, \text{ and Hyp. 3})
\end{aligned} \tag{28}$$

for positive constants c_1 and c'_1 independent of h and Δt .

We evaluate $a_1 \tilde{a}_1$. Let $U^\infty := \|u\|_{C([0, T]; C(\bar{\mathcal{Q}}; \mathbb{R}^d))} = \max\{|u_k(x, t)|; x \in \bar{\mathcal{Q}}, t \in [0, T], k = 1, 2\}$. From $y_1 = [x_{i,j} - u^n(x_{i,j})\Delta t]_1 \in [i_0 h_1, (i_0 + 1)h_1]$, it holds that

$$(i - i_0 - 1)h_1 \leq u_1^n(x_{i,j})\Delta t \leq (i - i_0)h_1.$$

In the case of $i - i_0 - 1 \in \mathbb{N}$, from $h_1 \leq \frac{u_1^n(x_{i,j})\Delta t}{i - i_0 - 1} \leq U^\infty \Delta t$, we have $a_1 \tilde{a}_1 \leq h_1^2 \leq h_1 U^\infty \Delta t$. In the case of $i - i_0 - 1 = 0$, from $a_1 \leq h_1$ and $\tilde{a}_1 = u_1^n(x_{i,j})\Delta t \leq U^\infty \Delta t$, we have $a_1 \tilde{a}_1 \leq h_1 U^\infty \Delta t$. Hence, it holds that, for any case,

$$a_1 \tilde{a}_1 \leq h_1 U^\infty \Delta t.$$

Since it holds that $a_2 \tilde{a}_2 \leq h_2 U^\infty \Delta t$ similarly, we obtain

$$a_1 \tilde{a}_1 + a_2 \tilde{a}_2 \leq 2h U^\infty \Delta t, \quad (29)$$

where this estimate holds also for $(k, l) = (i_0 + 1, j_0), (i_0, j_0 + 1), (i_0 + 1, j_0 + 1)$ similarly. Combining (28) and (29) with (27), we have, for a positive constant c_2 independent of h and Δt ,

$$\frac{2}{\Delta t} \left[(\Pi_h^{(1)} \zeta - \zeta) \circ X_1^n \right](x) \leq c_2 U^\infty h \|\zeta\|_{C([0, T]; C^2(\bar{\Omega}; \mathbb{R}^{d \times d}))} = O(h),$$

which implies the former equality in (26) with $p = 1$, and the latter is obtained similarly. Thus, we get (24) with $p = 1$.

In the case of $p = 2$, the result, i.e., (24) with $p = 2$, are obtained similarly by taking into account the next identity,

$$\left[(\Pi_h^{(2)} \zeta - \zeta) \circ X_1^n \right](x) = \sum_{(k, l) \in \Lambda^{(2)}(y)} \int_0^1 ds_1 \int_0^{s_1} ds_2 \int_0^{s_2} \left([(x_{k,l} - y) \cdot \nabla]^3 \zeta \right)(y + s_3(x_{k,l} - y)) ds_3 \varphi_{k,l}^{(2)}(y),$$

where $\Lambda^{(2)}(y) := \{(2i_* + p, 2j_* + q); p, q = 0, 1, 2\}$ for $i_* \in \{0, \dots, M_1\}$ and $j_* \in \{0, \dots, M_2\}$ satisfying $y \in [2i_* h_1, 2(i_* + 1)h_1] \times [2j_* h_2, 2(j_* + 1)h_2]$. \square

Remark 9. *It is obvious that*

$$\zeta^\nabla(x, t^n) = [\mathcal{A}_h^{n,(p)} \zeta](x) + O\left(\Delta t^2 + \frac{h^{p+1}}{\Delta t}\right) \quad (30)$$

for $x \in \bar{\Omega}_h$, $n \in \{2, \dots, N_T\}$ and $p = 1, 2$, since $\Pi_h^{(p)} \zeta$ has an accuracy of $O(h^{p+1})$. In fact, from the approximation property of $\Pi_h^{(p)} \zeta$, we have

$$\frac{2}{\Delta t} \left[(\Pi_h^{(p)} \zeta^{n-1} - \zeta^{n-1}) \circ X_1^n \right](x) = O\left(\frac{h^{p+1}}{\Delta t}\right), \quad (31a)$$

$$\frac{1}{2\Delta t} \left[(\Pi_h^{(p)} \zeta^{n-2} - \zeta^{n-2}) \circ \tilde{X}_1^n \right](x) = O\left(\frac{h^{p+1}}{\Delta t}\right), \quad (31b)$$

and the relation (30) is obtained by combining (31) with (25). Theorem 2 eliminates the negative order in Δt from (30) and ensures that we can take small Δt even for a fixed mesh size from a view point of accuracy.

4 Numerical schemes

In this section, we present finite difference schemes of second-order in time and of first- and second-order in space for problem (9) by using the ideas of discretizations given in Section 3.

Suppose that $u \in C^0([0, T]; C^1(\bar{\Omega}; \mathbb{R}^d))$ and $\zeta^0 \in C^0(\bar{\Omega}; \mathbb{R}_{\text{sym}}^{d \times d})$ are given, and that Hypotheses 1, 2 and 3 hold true. Our schemes are written in a unified form for $d = 1, 2, 3$ and $p = 1, 2$; find $\{\zeta_h^n \in V_h; n = 1, \dots, N_T\}$ such that

$$[\mathcal{A}_h^{n,(p)} \zeta_h](x) = F^n(x), \quad x \in \bar{\Omega}_h, \quad n \geq 1, \quad (32a)$$

$$\zeta_h^0(x) = \zeta^0(x), \quad x \in \bar{\Omega}_h, \quad (32b)$$

which are equivalent to

$$\frac{1}{2\Delta t} \left[3\zeta_h^n(x) - 4L_1^n(x) \left[(\Pi_h^{(p)} \zeta_h^{n-1}) \circ X_1^n \right](x) L_1^n(x)^\top \right]$$

$$+\tilde{L}_1^n(x)[(\Pi_h^{(p)}\zeta_h^{n-2})\circ\tilde{X}_1^n](x)\tilde{L}_1^n(x)^\top]=F^n(x), \quad x\in\bar{\Omega}_h, n\geq 2, \quad (33a)$$

$$\frac{1}{\Delta t}[\zeta_h^1(x)-L_1^1(x)[(\Pi_h^{(p)}\zeta_h^0)\circ X_1^1](x)L_1^1(x)^\top]=F^1(x), \quad x\in\bar{\Omega}_h, \quad (33b)$$

$$\zeta_h^0(x)=\zeta^0(x), \quad x\in\bar{\Omega}_h. \quad (33c)$$

The unified scheme (32) (equivalent to (33)) includes four schemes, i.e., $p = 1$ and 2 correspond to schemes of first- and second-order in space, respectively, and the spatial dimension $d (= 1, 2)$ is implicitly dealt in the symbols $\bar{\Omega}_h$ and V_h . An approximate initial value $\zeta_h^0 \in V_h$ is given by (33c). We find $\zeta_h^1 \in V_h$ from (33b) and $\zeta_h^n \in V_h$ for $n \geq 2$ from (33a). Here, we additionally provide practical form of (32):

$$\begin{aligned} \zeta_h^n(x) &= \frac{4}{3}L_1^n(x)[(\Pi_h^{(p)}\zeta_h^{n-1})\circ X_1^n](x)L_1^n(x)^\top \\ &\quad - \frac{1}{3}\tilde{L}_1^n(x)[(\Pi_h^{(p)}\zeta_h^{n-2})\circ\tilde{X}_1^n](x)\tilde{L}_1^n(x)^\top + \frac{2\Delta t}{3}F^n(x), \quad x\in\bar{\Omega}_h, n\geq 2, \end{aligned} \quad (34a)$$

$$\zeta_h^1(x) = L_1^1(x)[(\Pi_h^{(p)}\zeta_h^0)\circ X_1^1](x)L_1^1(x)^\top + \Delta tF^1(x), \quad x\in\bar{\Omega}_h, \quad (34b)$$

$$\zeta_h^0(x) = \zeta^0(x), \quad x\in\bar{\Omega}_h, \quad (34c)$$

which imply that scheme (32) is explicit.

Remark 10. From Hypotheses 1 and 2 and Remark 1, we have $\Gamma_{\text{in}} = \emptyset$ and $X_1(\Omega, t) = \tilde{X}_1(\Omega, t) = \Omega$ ($t \in [0, T]$), i.e., all of upwind points are in $\bar{\Omega}$. Hence, the functions $(\Pi_h^{(p)}\zeta_h^{n-1})\circ X_1^n$ ($n \geq 1$) and $(\Pi_h^{(p)}\zeta_h^{n-2})\circ\tilde{X}_1^n$ ($n \geq 2$) are well defined in $\bar{\Omega}$ for $p = 1, 2$.

Remark 11. In scheme (32), we employ the backward Euler method (33b) of first-order in time once to find ζ_h^1 needed in (33a) with $n = 2$. It is expected that there is no influence on the second-order convergence in time, cf. [38].

Remark 12. Suppose that Hypotheses 1 and 2 hold true. Then, under $F \in C(\bar{\Omega} \times [0, T]; \mathbb{R}^{d \times d})$ and $\zeta^0 \in C(\bar{\Omega}; \mathbb{R}^{d \times d})$, the scheme (32) preserves the symmetry, i.e., $\zeta_h^n(x)^\top = \zeta_h^n(x)$ ($x \in \bar{\Omega}_h$, $n = 0, \dots, N_T$) from the following. For $d = 1$, it is obvious, and let us consider $d = 2(, 3)$. $\zeta_h^0(x)$ ($x \in \bar{\Omega}_h$) is symmetric from the symmetry of ζ^0 . We show the symmetry of $\zeta_h^1(x)$ ($x \in \bar{\Omega}_h$). Noting (34b) and letting $A(x) = L_1^1(x)$, $B(x) = [(\Pi_h^{(p)}\zeta_h^0)\circ X_1^1](x)$, and $C(x) = \Delta tF^1(x)$, we have

$$\begin{aligned} \zeta_h^1(x)^\top &= [A(x)B(x)A(x)^\top + C(x)]^\top = A(x)B(x)^\top A(x)^\top + C(x)^\top \\ &= A(x)B(x)A(x)^\top + C(x) = \zeta_h^1(x), \end{aligned}$$

which implies symmetry of $\zeta_h^1(x)$ for $x \in \bar{\Omega}_h$, where we have used the fact that $B(x)$ and $C(x)$ are symmetric for the second equality from the last. For $n \geq 2$, the symmetry of $\zeta_h^n(x)$ is obtained similarly from (33a).

4.1 Schemes in one-dimensional space ($d = 1$)

In this subsection, we rewrite the finite difference scheme (32) in a unified form for $d = 1$ and $p = 1, 2$. We introduce simplified notations, $\zeta_i^n := \zeta_h^n(x_i)$, $u_i^n := u^n(x_i)$, $\nabla u_i^n := (\nabla u^n)(x_i)$, $F_i^n := F(x_i, t^n)$, $\Lambda_\Omega := \{0, \dots, N\}$, and $\Lambda_T := \{1, \dots, N_T\}$. The schemes are to find $\{\zeta_i^n \in \mathbb{R}; i \in \Lambda_\Omega, n \in \Lambda_T\}$ such that

$$\begin{aligned} \zeta_i^n &= \frac{4}{3}(1 + \Delta t\nabla u_i^n)^2[(\Pi_h^{(p)}\zeta_h^{n-1})\circ X_1^n](x_i) \\ &\quad - \frac{1}{3}(1 + 2\Delta t\nabla u_i^n)^2[(\Pi_h^{(p)}\zeta_h^{n-2})\circ\tilde{X}_1^n](x_i) + \frac{2\Delta t}{3}F_i^n, \quad i \in \Lambda_\Omega, n \geq 2, \end{aligned} \quad (35a)$$

$$\zeta_i^1 = (1 + \Delta t\nabla u_i^1)^2[(\Pi_h^{(p)}\zeta_h^0)\circ X_1^1](x_i) + \Delta tF_i^1, \quad i \in \Lambda_\Omega, \quad (35b)$$

$$\zeta_i^0 = \zeta^0(x_i), \quad i \in \Lambda_\Omega. \quad (35c)$$

We give the algorithm as follows:

Algorithm 1 ($d = 1$). Set $\bar{\Omega}_h = \{x_i \in \bar{\Omega}; i \in \Lambda_\Omega\}$ with $h = a/N$, and $\{\zeta_i^0; i \in \Lambda_\Omega\}$ by (35c) to get $\zeta_h^0 \in V_h$, where N is an even number and $M = N/2$ for $p = 2$.

Set $n = 1$.

For each $i \in \Lambda_\Omega$ do:

1. Compute $F_i^1, u_i^1, \nabla u_i^1$, and $y_i^1 := X_1^1(x_i) = x_i - \Delta t u_i^1$.
2. Compute $Z_i^{1,(p)} := [(I_h^{(p)} \zeta_h^0) \circ X_1^1](x_i) = (I_h^{(p)} \zeta_h^0)(y_i^1)$ according to (12) with $i_0 = \mathcal{I}(y_i^1; 0, a, N)$ for $p = 1$, or (13) with $k_0 = \mathcal{I}(y_i^1; 0, a, M)$ for $p = 2$.
3. Compute ζ_i^1 by (35b), which is equivalent to

$$\zeta_i^1 = (1 + \Delta t \nabla u_i^1)^2 Z_i^{1,(p)} + \Delta t F_i^1.$$

(Here, computation of $\zeta_h^1 \in V_h$ is completed.)

Set $n = 2$.

While $n \leq N_T$ do:

For each $i \in \Lambda_\Omega$ do:

1. Compute $F_i^n, u_i^n, \nabla u_i^n, y_i^n := X_1^n(x_i) = x_i - \Delta t u_i^n$, and $\tilde{y}_i^n := \tilde{X}_1^n(x_i) = x_i - 2\Delta t u_i^n$.
2. Compute $Z_i^{n,(p)} := [(I_h^{(p)} \zeta_h^{n-1}) \circ X_1^n](x_i) = (I_h^{(p)} \zeta_h^{n-1})(y_i^n)$ according to (12) with $i_0 = \mathcal{I}(y_i^n; 0, a, N)$ for $p = 1$, or (13) with $k_0 = \mathcal{I}(y_i^n; 0, a, M)$ for $p = 2$. Similarly, compute $\tilde{Z}_i^{n,(p)} := [(I_h^{(p)} \zeta_h^{n-2}) \circ \tilde{X}_1^n](x_i) = (I_h^{(p)} \zeta_h^{n-2})(\tilde{y}_i^n)$.
3. Compute ζ_i^n by (35a), which is equivalent to

$$\zeta_i^n = \frac{4}{3}(1 + \Delta t \nabla u_i^n)^2 z_i^{n,(p)} - \frac{1}{3}(1 + 2\Delta t \nabla u_i^n)^2 \tilde{Z}_i^{n,(p)} + \frac{2\Delta t}{3} F_i^n.$$

(Computation of $\zeta_h^n \in V_h$ is completed.)

Set $n = n + 1$.

4.2 Schemes in two-dimensional space ($d = 2$)

Similarly to the previous subsection, we rewrite the unified finite difference scheme (32) for $d = 2$ and $p = 1, 2$.

Let us introduce simplified notations, $\zeta_{i,j}^n := \zeta_h^n(x_{i,j})$, $u_{i,j}^n := u^n(x_{i,j})$, $\nabla u_{i,j}^n := (\nabla u^n)(x_{i,j})$, $F_{i,j}^n := F(x_{i,j}, t^n)$, and $\Lambda_\Omega := \{(i, j); i = 0, \dots, N_1, j = 0, \dots, N_2\}$. The schemes are to find $\{\zeta_{i,j}^n \in \mathbb{R}_{\text{sym}}^{2 \times 2}; (i, j) \in \Lambda_\Omega, n \in \Lambda_T\}$ such that

$$\begin{aligned} \zeta_{i,j}^n &= \frac{4}{3}[I + \Delta t(\nabla u_{i,j}^n)][(I_h^{(p)} \zeta_h^{n-1}) \circ X_1^n](x_{i,j})[I + \Delta t(\nabla u_{i,j}^n)]^\top \\ &\quad - \frac{1}{3}[I + 2\Delta t(\nabla u_{i,j}^n)][(I_h^{(p)} \zeta_h^{n-2}) \circ \tilde{X}_1^n](x_{i,j})[I + 2\Delta t(\nabla u_{i,j}^n)]^\top + \frac{2\Delta t}{3} F_{i,j}^n, \quad (i, j) \in \Lambda_\Omega, n \geq 2, \end{aligned} \quad (36a)$$

$$\zeta_{i,j}^1 = [I + \Delta t(\nabla u_{i,j}^1)][(I_h^{(p)} \zeta_h^0) \circ X_1^1](x_{i,j})[I + \Delta t(\nabla u_{i,j}^1)]^\top + \Delta t F_{i,j}^1, \quad (i, j) \in \Lambda_\Omega, \quad (36b)$$

$$\zeta_{i,j}^0 = \zeta^0(x_{i,j}), \quad (i, j) \in \Lambda_\Omega. \quad (36c)$$

We give an algorithm of schemes (36) for $d = 2$ and $p = 1, 2$, while the construction is analogous to Algorithm 1 for $d = 1$.

Algorithm 2 ($d = 2$). Set $\bar{\Omega}_h = \{x_{i,j} \in \bar{\Omega}; (i, j) \in \Lambda_\Omega\}$ with $h_i = a_i/N_i$ ($i = 1, 2$), and $\{\zeta_{i,j}^0; (i, j) \in \Lambda_\Omega\}$ by (36c) to get $\zeta_h^0 \in V_h$, where N_i ($i = 1, 2$) are even numbers and $M_i = N_i/2$ ($i = 1, 2$) for $p = 2$.

Set $n = 1$.

For each $(i, j) \in \Lambda_\Omega$ do:

1. Compute $F_{i,j}^1, u_{i,j}^1, \nabla u_{i,j}^1$, and $y_{i,j}^1 := X_1^1(x_{i,j}) = x_{i,j} - \Delta t u_{i,j}^1$.
2. Compute $Z_{i,j}^{1,(p)} := [(\Pi_h^{(p)} \zeta_h^0) \circ X_1^1](x_{i,j}) = (\Pi_h^{(p)} \zeta_h^0)(y_{i,j}^1)$ according to (14) with $i_0 = \mathcal{I}((y_{i,j}^1)_1; 0, a_1, N_1)$ and $j_0 = \mathcal{I}((y_{i,j}^1)_2; 0, a_2, N_2)$ for $p = 1$, or (15) with $k_0 = \mathcal{I}((y_{i,j}^1)_1; 0, a_1, M_1)$ and $l_0 = \mathcal{I}((y_{i,j}^1)_2; 0, a_2, M_2)$ for $p = 2$.
3. Compute $\zeta_{i,j}^1$ by (36b), which is equivalent to

$$\zeta_{i,j}^1 = [I + \Delta t(\nabla u_{i,j}^1)]Z_{i,j}^{1,(p)}[I + \Delta t(\nabla u_{i,j}^1)]^\top + \Delta t F_{i,j}^1.$$

(Here, computation of $\zeta_h^1 \in V_h$ is completed.)

Set $n = 2$.

While $n \leq N_T$ do:

For each $(i, j) \in \Lambda_\Omega$ do:

1. Compute $F_{i,j}^n, u_{i,j}^n, \nabla u_{i,j}^n, y_{i,j}^n := X_1^n(x_{i,j}) = x_{i,j} - \Delta t u_{i,j}^n$, and $\tilde{y}_{i,j}^n := \tilde{X}_1^n(x_{i,j}) = x_{i,j} - 2\Delta t u_{i,j}^n$.
2. Compute $Z_{i,j}^{n,(p)} := [(\Pi_h^{(p)} \zeta_h^{n-1}) \circ X_1^n](x_{i,j}) = (\Pi_h^{(p)} \zeta_h^{n-1})(y_{i,j}^n)$ according to (14) with $i_0 = \mathcal{I}((y_{i,j}^n)_1; 0, a_1, N_1)$ and $j_0 = \mathcal{I}((y_{i,j}^n)_2; 0, a_2, N_2)$ for $p = 1$, or (15) with $k_0 = \mathcal{I}((y_{i,j}^n)_1; 0, a_1, M_1)$ and $l_0 = \mathcal{I}((y_{i,j}^n)_2; 0, a_2, M_2)$ for $p = 2$. Similarly, compute $\tilde{Z}_{i,j}^{n,(p)} := [(\Pi_h^{(p)} \zeta_h^{n-2}) \circ \tilde{X}_1^n](x_{i,j}) = (\Pi_h^{(p)} \zeta_h^{n-2})(\tilde{y}_{i,j}^n)$.
3. Compute $\zeta_{i,j}^n$ by (36a), which is equivalent to

$$\zeta_{i,j}^n = \frac{4}{3}[I + \Delta t(\nabla u_{i,j}^n)]Z_{i,j}^{n,(p)}[I + \Delta t(\nabla u_{i,j}^n)]^\top - \frac{1}{3}[I + 2\Delta t(\nabla u_{i,j}^n)]\tilde{Z}_{i,j}^{n,(p)}[I + 2\Delta t(\nabla u_{i,j}^n)]^\top + \frac{2\Delta t}{3}F_{i,j}^n.$$

(Computation of $\zeta_h^n \in V_h$ is completed.)

Set $n = n + 1$.

5 Numerical results

In this section, numerical results for problems with manufactured solutions are presented to observe experimental convergence orders of proposed schemes. In the following, we denote scheme (32) with $p = 1$ and $p = 2$ by (S1) and (S2), respectively. From Theorem 2, the expected orders of convergence are of $O(\Delta t^2 + h^p)$ for $p = 1, 2$. To see the experimental orders of convergence, the efficient choices of Δt for (S1) and (S2) are respectively $\Delta t = c\sqrt{h}$ and $\Delta t = c'h$, for positive constants c and c' . The choices of Δt for (S1) and (S2) lead to an expected order of convergence of $O(\Delta t^2)$ ($= O(h^p)$). In the computations below, as mentioned in Remark 3-(iii) and Remark 5-(iii), we employ a value of ζ_{in} at closest lattice point to an upwind point $X_1^n(x)$ or $\tilde{X}_1^n(x)$ for $x = x_i$ ($d = 1$) or $x_{i,j}$ ($d = 2$) when the upwind point is outside the domain, where the integer-valued index indicator function \mathcal{I} given by (11) is used.

For $\psi_h : \bar{\Omega}_h \rightarrow \mathbb{R}$ and $\phi_h = \{\phi_h^n : \bar{\Omega}_h \rightarrow \mathbb{R}; n = 1, \dots, N_T\}$, let $\|\cdot\|_{\ell^\infty(\bar{\Omega}_h)}$ and $\|\cdot\|_{\ell^\infty(\ell^\infty)}$ be norms defined by

$$\begin{aligned} \|\psi_h\|_{\ell^\infty(\bar{\Omega}_h)} &= \|\psi_h\|_{\ell^\infty(\bar{\Omega}_h; \mathbb{R})} := \max\{|\psi_h(x)|; x \in \bar{\Omega}_h\}, \\ \|\phi_h\|_{\ell^\infty(\ell^\infty)} &:= \max\{\|\phi_h^n\|_{\ell^\infty(\bar{\Omega}_h)}; n = 1, \dots, N_T\}. \end{aligned}$$

Let $E_{ij} = E_{ij}(\Delta t, h)$, $i, j = 1, \dots, d$, be errors between a numerical solution $\zeta_h = \{\zeta_h^n\}_{n=1}^{N_T} \subset V_h$ and a corresponding exact solution $\zeta \in C([0, T]; C(\bar{\Omega}; \mathbb{R}_{\text{sym}}^{d \times d}))$ defined by

$$E_{ij} = E_{ij}(\Delta t, h) := \left\| [\zeta_h]_{ij} - \zeta_{ij} \right\|_{\ell^\infty(\ell^\infty)}, \quad i, j = 1, \dots, d,$$

and E_{11} is denoted by E simply when $d = 1$.

Remark 13. To solve the problems proposed in this Section, we are assuming a defined source term and a prescribed velocity field. In addition, we need to establish at least one initial condition and a wall condition where we can call the flow inlet. The initial condition $\zeta_{\text{in}}^0(x)$ is directly derived from the exact solution $\zeta_{\text{exact}}(x, 0)$. The boundary condition is computed assuming a Dirichlet-type condition, i.e., we use the exact solution $\zeta_{\text{in}} = \zeta_{\text{exact}}^n(x_0)$ at the first point of the boundary for a positive velocity field (if $u^n(x) < 0$ then the inlet of the domain is located on the opposite side, making us consider $\zeta_{\text{exact}}^n(x_N)$). Therefore, when we have the case described in Fig. 3, the interpolated point $X_1^n(x_0)$ at previous time is outside the domain; thus we have imposed the boundary condition $\zeta_{\text{in}}^n(x) = \zeta_{\text{exact}}^n(x)$.

For the opposite side of the domain as represented by Fig. 4, we do not impose any wall conditions, since our method can also be used to update the value of unknown function $\zeta_{\text{in}}^n(x_N)$ on the outflow wall. In addition, it is also possible to assume a Neumann boundary condition on this wall and then we apply the method until x_{N-1} and update the last point as in an explicit scheme $\zeta_{\text{in}}^n(x_N) = \zeta_{\text{in}}^n(x_{N-1})$.

More details about the implementation of these strategies can be found in Appendix A.3.

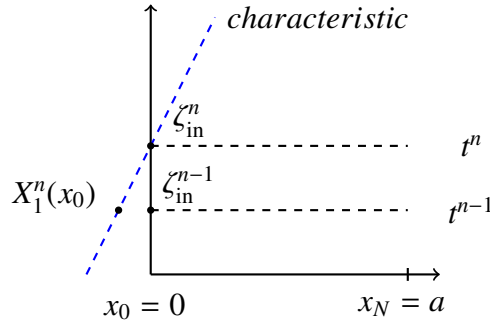


Fig. 3: Sketch of the wall treatment for unknown boundary condition.

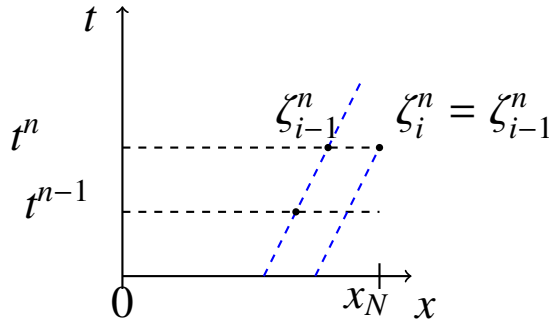


Fig. 4: Sketch of the wall treatment for Neumann boundary condition.

5.1 Examples in one-dimensional space ($d = 1$)

We consider the next example in one-dimensional space.

Example 1 ($d = 1$). In problem (9), let $d = 1$, $\Omega = (0, 1)$ and $T = 1$. We consider three functions for the velocity:

$$(i) u(x, t) = t, \quad (ii) u(x, t) = x + t, \quad (iii) u(x, t) = \sin(x + t),$$

which imply $\Gamma_{\text{in}} = \{0\}$ ($t \in (0, T]$). The functions F , ζ_{in} and ζ^0 are given so that the exact solution is

$$\zeta(x, t) = \sin(x + t) + 2.$$

We solve Example 1 by (S1) with $\Delta t = c\sqrt{h}$ for $c = 1/50$ and (S2) with $\Delta t = c'h$ for $c' = 1$, where the mesh is constructed for $h = 1/N$ with $N = 10, 20, 40, 80, 160$ and 320 , the constants c and c' are as larger as possible in order to numerically verify the convergence order of the temporal discretizations. Tables 1 and 2 show the values of error E and their slopes in Δt . According to the results in the tables, we can confirm that (S1) and (S2) are of second-order in Δt for the three cases of velocity, (i), (ii) and (iii). These results are consistent with the theoretical results in Theorem 2.

Table 1: Example 1 by (S1) with $\Delta t = c\sqrt{h}$ ($c = 1/50$): Values of E and their slopes in Δt .

| N | (i) | | (ii) | | (iii) | |
|-----|-----------------------|-------|-----------------------|-------|-----------------------|-------|
| | E | Slope | E | Slope | E | Slope |
| 10 | 1.54×10^{-2} | – | 3.45×10^{-2} | – | 2.11×10^{-2} | – |
| 20 | 8.07×10^{-3} | 1.86 | 1.83×10^{-2} | 1.87 | 1.11×10^{-2} | 1.86 |
| 40 | 4.15×10^{-3} | 1.92 | 9.38×10^{-3} | 1.92 | 5.69×10^{-3} | 1.92 |
| 80 | 2.10×10^{-3} | 1.96 | 4.75×10^{-3} | 1.96 | 2.88×10^{-3} | 1.96 |
| 160 | 1.06×10^{-3} | 1.98 | 2.39×10^{-3} | 1.98 | 1.45×10^{-3} | 1.98 |
| 320 | 5.31×10^{-4} | 1.99 | 1.13×10^{-3} | 2.16 | 7.27×10^{-4} | 1.99 |

Table 2: Example 1 by (S2) with $\Delta t = h$ ($c' = 1$): Values of E and their slopes in Δt .

| N | (i) | | (ii) | | (iii) | |
|-----|-----------------------|-------|-----------------------|-------|-----------------------|-------|
| | E | Slope | E | Slope | E | Slope |
| 10 | 4.65×10^{-3} | – | 8.05×10^{-2} | – | 1.65×10^{-2} | – |
| 20 | 1.11×10^{-3} | 2.07 | 2.19×10^{-2} | 1.88 | 5.45×10^{-3} | 1.60 |
| 40 | 2.68×10^{-4} | 2.04 | 5.63×10^{-3} | 1.96 | 1.53×10^{-3} | 1.84 |
| 80 | 6.59×10^{-5} | 2.03 | 1.42×10^{-3} | 1.98 | 4.02×10^{-4} | 1.93 |
| 160 | 1.63×10^{-5} | 2.01 | 3.58×10^{-4} | 1.99 | 1.03×10^{-4} | 1.97 |
| 320 | 4.06×10^{-6} | 2.01 | 8.96×10^{-5} | 2.00 | 2.61×10^{-5} | 1.98 |

In order to numerically verify that our methodology is stable for small time-steps, we have fixed a coarse mesh $h = 1/40$ and the finest mesh $h = 1/320$ simulating the reduction of the time-step as $\Delta t(k) = \frac{\sqrt{h}/50}{2^k}$ for the first-order scheme and as $\Delta t(k) = \frac{h}{2^k}$ for the second-order method. Results for (S1) in Table 3 while in Table 4 we have described the results for (S2).

According to these tables, we can confirm that our methodologies, first- and second-order spatial discretization schemes, are unconditionally stable since the errors are decreasing as Δt is reduced. It is important to highlight that error for the smallest time-step in Table 4 for $h = 1/40$ is approximately two order smaller than the error of the largest time-step, confirming the good stability property of the second-order scheme.

5.2 Examples for the two-dimensional case ($d = 2$)

We set the next example in two-dimensional space.

Example 2 ($d = 2$). In problem (9), let $d = 2$, $\Omega = (0, 1)^d$ and $T = 1$. We consider three functions for the velocity:

$$(i) u(x, t) = (t, t)^\top, \quad (ii) u(x, t) = (x_1 + t, x_2 + t)^\top, \\ (iii) u(x, t) = (\sin(x_1 + x_2 + t), \sin(x_1 + x_2 + t))^\top,$$

which imply $\Gamma_{\text{in}} = \{(s, 0)^\top \in \partial\Omega; s \in [0, 1]\} \cup \{(0, s)^\top \in \partial\Omega; s \in [0, 1]\}$ ($t \in (0, T)$). The functions F , ζ_{in} and ζ^0 are

Table 3: Example 1 by (S1): reducing the time-step as $\Delta t(k) = \frac{\sqrt{h}/50}{2^k}$.

| $h = 0.025$ | | |
|----------------|-----------------------|--------------------------|
| k | Δt | $Error$ |
| 0 | 3.16×10^{-3} | 1.18375×10^{-2} |
| 1 | 1.58×10^{-3} | 1.08387×10^{-2} |
| 2 | 7.91×10^{-4} | 1.03445×10^{-2} |
| 3 | 3.95×10^{-4} | 1.01025×10^{-2} |
| 4 | 1.98×10^{-4} | 9.98198×10^{-3} |
| 5 | 9.88×10^{-5} | 9.92182×10^{-3} |
| 6 | 4.94×10^{-5} | 9.89128×10^{-3} |
| $h = 0.003125$ | | |
| k | Δt | $Error$ |
| 0 | 1.12×10^{-3} | 1.94633×10^{-3} |
| 1 | 5.59×10^{-4} | 1.57935×10^{-3} |
| 2 | 2.80×10^{-4} | 1.39709×10^{-3} |
| 3 | 1.40×10^{-4} | 1.30627×10^{-3} |
| 4 | 6.99×10^{-5} | 1.26087×10^{-3} |
| 5 | 3.49×10^{-5} | 1.23823×10^{-3} |
| 6 | 1.75×10^{-5} | 1.22691×10^{-3} |

Table 4: Example 1 by (S2): reducing the time-step as $\Delta t(k) = \frac{h}{2^k}$.

| $h = 0.025$ | | |
|----------------|-----------------------|-----------------------|
| k | Δt | $Error$ |
| 0 | 2.50×10^{-2} | 5.63×10^{-3} |
| 1 | 1.25×10^{-2} | 1.50×10^{-3} |
| 2 | 6.25×10^{-3} | 4.30×10^{-4} |
| 3 | 3.13×10^{-3} | 1.58×10^{-4} |
| 4 | 1.56×10^{-3} | 8.97×10^{-5} |
| 5 | 7.81×10^{-4} | 7.27×10^{-5} |
| 6 | 3.91×10^{-4} | 6.84×10^{-5} |
| $h = 0.003125$ | | |
| k | Δt | $Error$ |
| 0 | 3.13×10^{-3} | 8.96×10^{-5} |
| 1 | 1.56×10^{-3} | 2.34×10^{-5} |
| 2 | 7.81×10^{-4} | 6.64×10^{-6} |
| 3 | 3.91×10^{-4} | 2.41×10^{-6} |
| 4 | 1.95×10^{-4} | 1.36×10^{-6} |
| 5 | 9.77×10^{-5} | 1.10×10^{-6} |
| 6 | 4.88×10^{-5} | 1.03×10^{-6} |

given so that the exact solution is

$$\zeta(x, t) = \begin{bmatrix} \sin(x_1 + x_2 + t) + 2 & \sin(x_1 + x_2 + t) \\ \sin(x_1 + x_2 + t) & \sin(x_1 + x_2 + t) + 2 \end{bmatrix}.$$

We solve Example 2 by (S1) with $\Delta t = c\sqrt{h}$ for $c = 1/20$ and (S2) with $\Delta t = c'h$ for $c' = 1/10$, where the mesh is constructed for $h_1 = h_2 = h = 1/N$, i.e., $N_1 = N_2 = N$, with $N = 10, 20, 40$ and 80 . Tables 5 and 6 show the values of error E_{11} and their slopes in Δt . Slope results for E_{12} and E_{22} adopting different velocity fields (i), (ii) and (iii) are very similar to those obtained for E_{11} ; thus they are omitted here in order to save space. We can confirm that

(S1) and (S2) are of second-order in Δt in two-dimensional space for the three cases of velocity, (i), (ii) and (iii). These results are consistent with the theoretical results in Theorem 2.

Table 5: Example 2 by (S1) with $\Delta t = c\sqrt{h}$ ($c = 1/20$): Values of E_{11} and their slopes in Δt .

| N | (i) | | (ii) | | (iii) | |
|-----|-----------------------|-------|-----------------------|-------|-----------------------|-------|
| | E_{11} | Slope | E_{11} | Slope | E_{11} | Slope |
| 10 | 3.87×10^{-2} | – | 3.84×10^{-2} | – | 3.87×10^{-2} | – |
| 20 | 1.98×10^{-2} | 1.94 | 1.96×10^{-2} | 1.94 | 1.98×10^{-2} | 1.94 |
| 40 | 9.99×10^{-3} | 1.97 | 9.94×10^{-3} | 1.97 | 9.99×10^{-3} | 1.97 |
| 80 | 5.03×10^{-3} | 1.98 | 5.01×10^{-3} | 1.98 | 5.03×10^{-3} | 1.98 |

Table 6: Example 2 by (S2) with $\Delta t = c'h$ ($c' = 1/10$): Values of E_{11} and their slopes in Δt .

| N | (i) | | (ii) | | (iii) | |
|-----|-----------------------|-------|-----------------------|-------|-----------------------|-------|
| | E_{11} | Slope | E_{11} | Slope | E_{11} | Slope |
| 10 | 2.07×10^{-4} | – | 2.18×10^{-3} | – | 9.79×10^{-4} | – |
| 20 | 5.10×10^{-5} | 2.02 | 5.35×10^{-4} | 2.02 | 2.53×10^{-4} | 1.95 |
| 40 | 1.27×10^{-5} | 2.00 | 1.32×10^{-4} | 2.02 | 6.39×10^{-5} | 1.98 |
| 80 | 3.17×10^{-6} | 2.00 | 3.27×10^{-5} | 2.01 | 1.61×10^{-5} | 1.99 |

5.3 The Oldroyd-B constitutive equation in two-dimensional space

We apply our approximations of the upper-convected time derivative of second-order in time (24) in Theorem 2 for solving a problem governed by the Oldroyd-B constitutive equation in two-dimensional space; find $\zeta : \Omega \times (0, T) \rightarrow \mathbb{R}_{\text{sym}}^{d \times d}$ such that

$$\zeta + Wi \overset{\nabla}{\zeta} = 2(1 - \beta)D(u) + F \quad \text{in } \Omega \times (0, T), \quad (37a)$$

$$\zeta = \zeta_{\text{in}} \quad \text{on } \Gamma_{\text{in}} \times (0, T), \quad (37b)$$

$$\zeta = \zeta^0 \quad \text{in } \Omega, \text{ at } t = 0. \quad (37c)$$

The scheme to solve problem (37) is to find $\{\zeta_h^n \in V_h; n = 1, \dots, N_T\}$ such that

$$\zeta_h^n(x) + Wi[\mathcal{A}_h^{n,(p)}\zeta_h](x) = 2(1 - \beta)D(u^n)(x) + F^n(x), \quad x \in \bar{\Omega}_h, n \geq 1, \quad (38a)$$

$$\zeta_h^0(x) = \zeta^0(x), \quad x \in \bar{\Omega}_h, \quad (38b)$$

where $\mathcal{A}_h^{n,(p)}\zeta_h : \bar{\Omega}_h \rightarrow \mathbb{R}_{\text{sym}}^{d \times d}$ is the function defined already by (23). When an upwind point is outside the domain, we employ a value of ζ_{in} at closest lattice point to the upwind point similarly to the case of scheme (32) as mentioned in Remark 5-(iii). In the following, scheme (38) with $p = 1$ and $p = 2$ for problem (37) are called (S1)' and (S2)', respectively.

We set two examples below:

Example 3 ($d = 2$). In problem (37), let $d = 2$, $\Omega = (0, 1)^d$, $T = 1$ and $\beta = 1/9$. We consider six values of the Weissenberg number Wi ,

$$Wi = 0.025, 1, 5, 10, 50, 100,$$

and the following function for the velocity field:

$$u(x, t) = (\sin(x_1 + x_2 + t), \sin(x_1 + x_2 + t))^T,$$

which implies $\Gamma_{\text{in}} = \{(s, 0)^\top \in \partial\Omega; s \in [0, 1]\} \cup \{(0, s)^\top \in \partial\Omega; s \in [0, 1]\}$. The functions F , ζ_{in} and ζ^0 are given so that the exact solution is

$$\zeta(x, t) = \begin{bmatrix} \sin(x_1 + x_2 + t) + 2 & \sin(x_1 + x_2 + t) \\ \sin(x_1 + x_2 + t) & -\sin(x_1 + x_2 + t) + 2 \end{bmatrix}.$$

Example 4 ($d = 2$, [57]). In problem (37), let $d = 2$, $\Omega = (0, 1)^d$, $T = 0.5$, $\beta = 0.75$ and $Wi = 0.25$. We consider the following function for the velocity field:

$$u(x, t) = (\exp(-0.1t) \sin(\pi x_1), -\pi \exp(-0.1t) x_2 \cos(\pi x_1))^\top,$$

which implies $\Gamma_{\text{in}} = \{(s, 0)^\top \in \partial\Omega; s \in [0, 1]\} \cup \{(0, s)^\top \in \partial\Omega; s \in [0, 1]\}$. The functions F , ζ_{in} and ζ^0 are given so that the exact solution is

$$\zeta(x, t) = \begin{bmatrix} \exp(-0.1t) \sin(\pi x_1) & -\pi \exp(-0.1t) x_2 \cos(\pi x_1) \\ -\pi \exp(-0.1t) x_2 \cos(\pi x_1) & \exp(-0.1t) \sin(\pi x_1) \cos(\pi x_2) \end{bmatrix}.$$

We solve Example 3 by (S1)' with $\Delta t = c\sqrt{h}$ for $c = 1/50$ and (S2)' with $\Delta t = c'h$ for $c' = 1/5$, where the mesh is constructed for $h_1 = h_2 = h = 1/N$, i.e., $N_1 = N_2 = N$, with $N = 10, 20, 40$ and 80 . In order to further investigate the errors and the orders of convergence of the schemes for solving problem (37), we give the results for the three different components ζ_{11} , ζ_{12} and ζ_{22} . Tables 7 and 8 show the results by (S1)' and (S2)', respectively, for $Wi = 0.025$. From a quantitative point of view, the results are consistent with the theoretical results in Theorem 2.

Table 7: Example 3 by (S1)' with $\Delta t = c\sqrt{h}$ ($c = 1/50$): Values of each tensor entry E_{11}, E_{12}, E_{22} and their slopes in Δt for $Wi = 0.025$.

| N | E_{11} | Slope | E_{12} | Slope | E_{22} | Slope |
|-----|-----------------------|-------|-----------------------|-------|-----------------------|-------|
| 10 | 2.03×10^{-3} | – | 2.03×10^{-3} | – | 2.03×10^{-3} | – |
| 20 | 1.02×10^{-3} | 1.99 | 1.02×10^{-3} | 1.99 | 1.02×10^{-3} | 1.99 |
| 40 | 5.11×10^{-4} | 1.99 | 5.11×10^{-4} | 1.99 | 5.11×10^{-4} | 1.99 |
| 80 | 2.56×10^{-4} | 1.99 | 2.56×10^{-4} | 1.99 | 2.56×10^{-4} | 1.99 |

Table 8: Example 3 by (S2)' with $\Delta t = c'h$ ($c' = 1/5$): Values of each tensor entry E_{11}, E_{12}, E_{22} and their slopes in Δt for $Wi = 0.025$.

| N | E_{11} | Slope | E_{12} | Slope | E_{22} | Slope |
|-----|-----------------------|-------|-----------------------|-------|-----------------------|-------|
| 10 | 7.62×10^{-5} | – | 7.24×10^{-5} | – | 7.62×10^{-5} | – |
| 20 | 1.89×10^{-6} | 2.02 | 1.80×10^{-6} | 2.01 | 1.89×10^{-5} | 2.02 |
| 40 | 4.75×10^{-6} | 1.99 | 4.57×10^{-6} | 1.98 | 4.75×10^{-6} | 1.99 |
| 80 | 1.21×10^{-6} | 1.97 | 1.17×10^{-6} | 1.96 | 1.21×10^{-6} | 1.97 |

A computational challenge in viscoelastic fluid flows is the application of high values of the Weissenberg number, i.e., $Wi > 1$. In fact, the *infamous* High Weissenberg Number Problem [18, 23, 33] depends of some particular factors on viscoelastic flows, as for instance, domain geometry, boundary conditons, fluid type, mesh size, etc. In summary, this instability is related to the unbounded values of the stress tensor during the transient solution resulting in the fail of the numerical methods. It is important to highlight that some classical methods, i.e. without stabilization techniques, have failed for $Wi = O(1)$ exhibiting numerical oscillations of the solution. Roughly speaking, the High Weissenberg Number Problem can be interpreted according to a critical value of the Weissenberg number, Wi_{crit} , which the numerical solution is boundly maintained during the simulation of the classical constitutive formulations. For example, considering the traditional Oldroyd-B model, Fattal and Kupferman [18] described $Wi_{\text{crit}} \approx 0.5$ for the cavity flow while Oliveira and Miranda [40] pointed out $Wi_{\text{crit}} \approx 1$ for unsteady

viscoelastic flow past bounded cylinders. Moreover, Walters and Webster [58] presented results for the 4 : 1 contraction problem with the critical Weissenberg number near to 3. Therefore, there is an effort of the researchers to circumvent the High Weissenberg Number Problem developing new formulations that can be stable in simulations with $Wi > Wi_{crit}$.

It is important to highlight that the schemes presented in this current work can deal with high values of Wi without the need to employ stabilization strategies. To test the accuracy of (S2)', we vary the values of Weissenberg number as $Wi = 1, 5, 10, 50, 100$ in Example 3 and the results are presented in Table 9. The main focus for varying the Weissenberg number is to verify the ability of (S2)' for dealing with the Oldroyd-B constitutive equation defined on the context of high elasticity. From the results presented in Table 9, we can notice that the numerical order of convergence of (S2)' is of second-order in both time and space, and that the effect of varying the Weissenberg number is not significant for this example.

Table 9: Example 3 by (S2)' with $\Delta t = c'h$ ($c' = 1/5$) and different values of Wi number.

| $Wi = 1.0$ | | | | | | |
|------------|-----------------------|-------|-----------------------|-------|-----------------------|-------|
| N | E_{11} | Slope | E_{12} | Slope | E_{22} | Slope |
| 10 | 1.55×10^{-3} | – | 1.06×10^{-3} | – | 5.54×10^{-4} | – |
| 20 | 4.23×10^{-4} | 1.88 | 2.93×10^{-4} | 1.85 | 1.48×10^{-4} | 1.91 |
| 40 | 1.09×10^{-4} | 1.95 | 7.65×10^{-5} | 1.94 | 3.79×10^{-5} | 1.96 |
| 80 | 2.77×10^{-5} | 1.98 | 1.95×10^{-5} | 1.98 | 9.58×10^{-6} | 1.99 |
| $Wi = 5$ | | | | | | |
| N | E_{11} | Slope | E_{12} | Slope | E_{22} | Slope |
| 10 | 1.97×10^{-3} | – | 1.37×10^{-3} | – | 7.13×10^{-4} | – |
| 20 | 5.36×10^{-4} | 1.87 | 3.80×10^{-4} | 1.85 | 1.97×10^{-4} | 1.86 |
| 40 | 1.39×10^{-4} | 1.95 | 9.90×10^{-5} | 1.94 | 5.14×10^{-5} | 1.94 |
| 80 | 3.51×10^{-5} | 1.98 | 2.52×10^{-5} | 1.98 | 1.31×10^{-5} | 1.97 |
| $Wi = 10$ | | | | | | |
| N | E_{11} | Slope | E_{12} | Slope | E_{22} | Slope |
| 10 | 2.03×10^{-3} | – | 1.42×10^{-3} | – | 7.38×10^{-4} | – |
| 20 | 5.54×10^{-4} | 1.87 | 3.93×10^{-4} | 1.85 | 2.04×10^{-4} | 1.85 |
| 40 | 1.43×10^{-4} | 1.94 | 1.03×10^{-4} | 1.94 | 5.35×10^{-5} | 1.93 |
| 80 | 3.63×10^{-5} | 1.98 | 2.61×10^{-5} | 1.98 | 1.36×10^{-5} | 1.97 |
| $Wi = 50$ | | | | | | |
| N | E_{11} | Slope | E_{12} | Slope | E_{22} | Slope |
| 10 | 2.08×10^{-3} | – | 1.46×10^{-3} | – | 7.59×10^{-4} | – |
| 20 | 5.69×10^{-4} | 1.87 | 4.05×10^{-4} | 1.85 | 2.11×10^{-4} | 1.85 |
| 40 | 1.47×10^{-4} | 1.95 | 1.06×10^{-4} | 1.94 | 5.53×10^{-5} | 1.93 |
| 80 | 3.72×10^{-5} | 1.98 | 2.68×10^{-5} | 1.98 | 1.41×10^{-5} | 1.97 |
| $Wi = 100$ | | | | | | |
| N | E_{11} | Slope | E_{12} | Slope | E_{22} | Slope |
| 10 | 2.09×10^{-3} | – | 1.46×10^{-3} | – | 7.62×10^{-4} | – |
| 20 | 5.71×10^{-4} | 1.87 | 4.06×10^{-4} | 1.85 | 2.12×10^{-4} | 1.85 |
| 40 | 1.48×10^{-4} | 1.95 | 1.06×10^{-4} | 1.94 | 5.55×10^{-5} | 1.93 |
| 80 | 3.74×10^{-5} | 1.98 | 2.69×10^{-5} | 1.98 | 1.42×10^{-5} | 1.97 |

Finally, example 4 employs the manufactured solution used by Venkatesan and Ganesan [57]. Notice that in this study we are investigating the numerical behavior of the schemes for non-homogeneous boundary conditions in parts of the domain. Table 10 describes the results for Example 4 by (S2)' with $\Delta t = c'h$ for $c' = 1/10$, where the mesh is constructed for $h_1 = h_2 = h = 1/N$, i.e., $N_1 = N_2 = N$, with $N = 10, 20, 40$ and 80 . From this table we can see that these results are consistent with our truncation error analysis in Theorem 2.

Table 10: Example 4 by (S2)' with $\Delta t = c'h$ ($c' = 1/10$): Values of each tensor entry E_{11}, E_{12}, E_{22} and their slopes in Δt for $Wi = 0.25$ and $\beta = 0.75$.

| N | E_{11} | Slope | E_{12} | Slope | E_{22} | Slope |
|-----|-----------------------|-------|-----------------------|-------|-----------------------|-------|
| 10 | 4.10×10^{-3} | – | 7.64×10^{-2} | – | 1.98×10^{-2} | – |
| 20 | 1.02×10^{-3} | 2.01 | 2.11×10^{-3} | 1.86 | 5.19×10^{-3} | 1.93 |
| 40 | 2.82×10^{-4} | 1.86 | 5.83×10^{-4} | 1.85 | 1.32×10^{-3} | 1.97 |
| 80 | 7.47×10^{-5} | 1.91 | 1.54×10^{-4} | 1.92 | 3.30×10^{-4} | 2.00 |

6 Conclusions

The application of the generalized Lie derivative (GLD) for constructing schemes to deal with the upper-convected time derivative is an alternative form in the numerical solution of constitutive equations. In spite of the success of this strategy firstly proposed by Lee and Xu [25], to the best knowledge of the authors, the methodology was only applied in the context of finite elements. In this work, we have combined a Lagrangian framework with GLD to develop new second-order finite difference approximations for the upper-convected time derivative. Particularly, the schemes are constructed based on bilinear and biquadratic interpolation operators for solving a simple model in one- and two-dimensional spaces. The schemes are explicit and no CFL condition is required as the Lagrangian framework is employed. Truncation errors of $O(\Delta t^2 + h^p)$ ($p = 1, 2$) for the finite difference approximations of the the upper-convected time derivative have been proved. A numerical integration of composite functions may cause an instability in the case of Lagrangian finite element method, our schemes, however, do not have such instability since there is no numerical integration thanks to the finite difference method. According to our numerical results for simplified model equations, the new finite difference schemes can reach second-order of accuracy in time and space ($p = 2$) corroborating with the theoretical analysis. Moreover, the proposed strategy has been also applied to solve a two-dimensional Oldroyd-B constitutive equation subjected to a prescribed velocity field. The results have been very satisfactory since the increasing of the Weissenberg number did not influence the good properties of accuracy and stability of the finite difference approximations. As a future work, we intend to extend our schemes for solving viscoelastic fluid flows governed by different constitutive equations at high Weissenberg numbers.

Appendix

A.1 Proofs of properties in (5)

Firstly, we prove (5a). The second equality of (5a) is obtained immediately from the definition of L in (4) as

$$L_{ij}(x, t; t_1, t_1) = \left[\frac{\partial}{\partial z_j} X_i(z, t_1; t_1) \right]_{|z=X(x,t,t_1)} = \left[\frac{\partial}{\partial z_j} z_i \right]_{|z=X(x,t,t_1)} = [\delta_{ij}]_{|z=X(x,t,t_1)} = \delta_{ij},$$

where δ_{ij} ($i, j = 1, \dots, d$) is Kronecker's delta function. For the first equality of (5a), we prove

$$I = L(x, t; t_1, t_2)L(x, t; t_2, t_1). \quad (\text{A.1})$$

Let $x \in \bar{\mathcal{Q}}$ and $t_1, t_2 \in [0, T]$ be fixed arbitrarily. For any $y \in \bar{\mathcal{Q}}$, it holds that

$$y = X(X(y, t_2; t_1), t_1; t_2),$$

which is equivalent to

$$y_i = X_i(X(y, t_2; t_1), t_1; t_2), \quad i = 1, \dots, d. \quad (\text{A.2})$$

The differentiation of both sides of (A.2) with respect to y_j ($j = 1, \dots, d$) implies that

$$\delta_{ij} = \frac{\partial}{\partial y_j} (X_i(X(y, t_2; t_1), t_1; t_2)) = \sum_{k=1}^d \left[\frac{\partial}{\partial z_k} X_i(z, t_1; t_2) \right]_{|z=X(y, t_2; t_1)} \left[\frac{\partial}{\partial z_j} X_k(z, t_2; t_1) \right]_{|z=y}. \quad (\text{A.3})$$

Substituting $X(x, t; t_2)$ into y in (A.3) and using $X(X(x, t; t_2), t_2; t_1) = X(x, t; t_1)$, we get

$$\delta_{ij} = \sum_{k=1}^d \left[\frac{\partial}{\partial z_k} X_i(z, t_1; t_2) \right] \Big|_{z=X(x, t; t_1)} \left[\frac{\partial}{\partial z_j} X_k(z, t_2; t_1) \right] \Big|_{z=X(x, t; t_2)} = \sum_{k=1}^d L_{ik}(x, t; t_1, t_2) L_{kj}(x, t; t_2, t_1),$$

which implies (A.1). Thus, the first equality of (5a) holds true.

Secondly, we prove (5b). From the definition of L in (4), we have

$$\begin{aligned} \frac{\partial}{\partial s} L_{ij}(x, t; t_1, s) &= \left[\frac{\partial}{\partial s} \frac{\partial}{\partial z_j} X_i(z, t_1; s) \right] \Big|_{z=X(x, t; t_1)} \\ &= \left[\frac{\partial}{\partial z_j} \frac{\partial}{\partial s} X_i(z, t_1; s) \right] \Big|_{z=X(x, t; t_1)} = \left[\frac{\partial}{\partial z_j} u_i(X(z, t_1; s), s) \right] \Big|_{z=X(x, t; t_1)} \\ &= \left[\sum_{k=1}^d \frac{\partial u_i}{\partial x_k}(X(z, t_1; s), s) \frac{\partial}{\partial z_j} X_k(z, t_1; s) \right] \Big|_{z=X(x, t; t_1)} = \sum_{k=1}^d \frac{\partial u_i}{\partial x_k}(X(x, t; s), s) \left[\frac{\partial}{\partial z_j} X_k(z, t_1; s) \right] \Big|_{z=X(x, t; t_1)} \\ &= \sum_{k=1}^d [\nabla u]_{ik}(X(x, t; s), s) L_{kj}(x, t; t_1, s), \end{aligned}$$

which implies (5b).

Finally, we prove (5c). Property (5a) gives an identity,

$$I = L(x, t; t_1, s) L(x, t; s, t_1).$$

Considering the derivative of the identity above with respect to s , we have

$$\begin{aligned} 0 &= \frac{\partial}{\partial s} [L(x, t; t_1, s) L(x, t; s, t_1)] = \left[\frac{\partial}{\partial s} L(x, t; t_1, s) \right] L(x, t; s, t_1) + L(x, t; t_1, s) \left[\frac{\partial}{\partial s} L(x, t; s, t_1) \right] \\ &= (\nabla u)(X(x, t; s), s) L(x, t; t_1, s) L(x, t; s, t_1) + L(x, t; t_1, s) \left[\frac{\partial}{\partial s} L(x, t; s, t_1) \right] \quad (\text{by (5b)}) \\ &= (\nabla u)(X(x, t; s), s) + L(x, t; t_1, s) \left[\frac{\partial}{\partial s} L(x, t; s, t_1) \right] \quad (\text{by (5a)}), \end{aligned}$$

which completes the proof of (5c) as

$$\frac{\partial}{\partial s} L(x, t; s, t_1) = -L(x, t; t_1, s)^{-1} (\nabla u)(X(x, t; s), s) = -L(x, t; s, t_1) (\nabla u)(X(x, t; s), s) \quad (\text{by (5a)}).$$

A.2 Proof of (8)

For the sake of simplicity, we employ simple notations, $L(\cdot, \cdot) = L(x, t; \cdot, \cdot)$ and $X = X(x, t; \cdot)$, as there is no confusion. From the definition of the generalized Lie derivative in (7) and the properties of L in (5), we have

$$\begin{aligned} (\mathcal{L}_u \zeta)(x, t) &= (\mathcal{L}_u \zeta)(X(s), s) \Big|_{s=t} = L(t, s) \frac{\partial}{\partial s} \left[L(s, t) \zeta(X(s), s) L(s, t)^\top \right] \Big|_{s=t} \\ &= L(t, s) \left[\left(\frac{\partial}{\partial s} L(s, t) \right) \zeta(X(s), s) L(s, t)^\top + L(s, t) \left(\frac{\partial}{\partial s} \zeta(X(s), s) \right) L(s, t)^\top + L(s, t) \zeta(X(s), s) \left(\frac{\partial}{\partial s} L(s, t)^\top \right) \right] \Big|_{s=t} \\ &= L(t, s) \left[\left(-L(s, t) (\nabla u)(X(s), s) \right) \zeta(X(s), s) L(s, t)^\top + L(s, t) \frac{D\zeta}{Dt}(X(s), s) L(s, t)^\top \right. \\ &\quad \left. + L(s, t) \zeta(X(s), s) \left(-L(s, t) (\nabla u)(X(s), s) \right)^\top \right] \Big|_{s=t} \\ &= L(t, s) \left[-L(s, t) (\nabla u)(X(s), s) \zeta(X(s), s) L(s, t)^\top + L(s, t) \frac{D\zeta}{Dt}(X(s), s) L(s, t)^\top \right] \end{aligned}$$

$$\begin{aligned}
& -L(s, t)\zeta(X(s), s)(\nabla u)^\top(X(s), s)L(s, t)^\top \Big] L(t, s)^\top \Big|_{s=t} \\
& = \left[-(\nabla u)(X(s), s)\zeta(X(s), s) + \frac{D\zeta}{Dt}(X(s), s) - \zeta(X(s), s)(\nabla u)^\top(X(s), s) \right] \Big|_{s=t} \\
& = -(\nabla u)(x, t)\zeta(x, t) + \frac{D\zeta}{Dt}(x, t) - \zeta(x, t)(\nabla u)^\top(x, t),
\end{aligned}$$

which completes the proof of (8).

A.3 Pseudo-codes for the proposed scheme

The Algorithm A.1 contains the steps of the interpolation process for the evaluated function on the characteristic curve at a previous time.

The main algorithm (see Algorithm A.2) has all declarations and computations used to update the numerical solution on time.

Algorithm A.1 Interpolation algorithm

Require: $y_{i,j}^n, h_d (d = 1, 2), (i, j), \Lambda_\Omega, p, x_{i,j}, \bar{\Omega}_h$ and ζ_h .

- 1: Calculate the index on the discretized mesh $(i_0, j_0) \in \Lambda_\Omega$, i.e., $index(y_{i,j}^n) = (i_0, j_0)$.
- 2: Calculate $\eta_{i_0}^{(p)}$ and $\eta_{j_0}^{(p)}$
- 3: **if** $p = 1$ **then**

$$\eta_{i_0}^{(1)}(x; h_1) := \begin{cases} \frac{x - x_{i_0-1}}{h_1} & (x \in [x_{i_0-1}, x_{i_0})), \\ \frac{x_{i_0+1} - x}{h_1} & (x \in [x_{i_0}, x_{i_0+1}]), \\ 0 & (\text{otherwise}), \end{cases}$$

and the same to calculate the function $\eta_{j_0}^{(1)}$ using the index j_0 and space-step h_1 .

- 4: **else**

$$\eta_{i_0}^{(2)}(x; h_1) := \begin{cases} \frac{x - x_{i_0-1}}{h_1} \cdot \frac{x - x_{i_0-2}}{2h_1} & (x \in [x_{i_0-2}, x_{i_0})), \\ \frac{x_{i_0+1} - x}{h_1} \cdot \frac{x - x_{i_0+2}}{2h_1} & (x \in [x_{i_0}, x_{i_0+2}]), \\ 0 & (\text{otherwise}), \end{cases}$$

and the again to compute the function $\eta_{j_0}^{(2)}$ using the index j_0 and space-step h_2 .

- 5: **end if**
- 6: Define the basis function $\varphi_{i_0, j_0}^{(p)}$ as

$$\varphi_{i_0, j_0}^{(p)}(y_{i,j}^n) := \eta_{i_0}^{(p)}(y_i^n; h_1)\eta_{j_0}^{(p)}(y_j^n; h_2).$$

- 7: Compute the interpolation of the given function ζ_h at $y_{i,j}^n$ by

$$Z_{i,j}^{1,(p)} := (\Pi_h^{(p)} \zeta_h)(y_{i,j}^n) = \sum_{x_{i,j} \in \Omega_h} \zeta_h(x_{i,j})\varphi_{i_0, j_0}^{(p)}(y_{i,j}^n).$$

return $Z_{i,j}^{1,(p)}$.

Algorithm A.2 Main algorithm

Require: The domain Ω with a_d ($d = 1, 2$), division numbers N_d ($d = 1, 2$), interpolation order p , final time T , time step Δt and the exact solution $\zeta_{\text{exact}}^n(x_{i,j})$.

- 1: Calculate $h_d = a_d/N_d$ ($d = 1, 2$) and $\bar{\Omega}_h$, where N_d ($d = 1, 2$) are even numbers and $M_d = N_d/2$ ($d = 1, 2$) for $p = 2$, the indexes domain $\Lambda_\Omega = \{(i, j); i = 0, \dots, N_1, j = 0, \dots, N_2\}$ and the number of time steps N_T .
- 2: Initialize the value $\zeta_{\text{in}}^n(x_{i,j}) = \zeta_{\text{exact}}^n(x_{i,j})$ for $n = 0$ with $(i, j) \in \Lambda_\Omega$ and $x_{i,j} \in \Gamma_{\text{in}} = \{(s, 0)^\top \in \partial\Omega; s \in [0, 1]\} \cup \{(0, s)^\top \in \partial\Omega; s \in [0, 1]\}$ ($t \in (0, T]$).

3: Define the functions $u_{i,j}^n$, $\nabla u_{i,j}^n$ and $F_{i,j}^n$.

4: Set $n = 1$.

5: **for** $(i, j) \in \Lambda_\Omega$ **do**

6: Calculate the interpolation point $y_{i,j}^1 := X_1^n(x_{i,j}) = x_{i,j} - u_{i,j}^1 \Delta t$.

7: **if** $(y_{i,j}^1 \notin \bar{\Omega})$ **then**

$$\zeta_{i,j}^1 = \zeta_{\text{in}}^1(x_{i,j}).$$

8: **else**

9: Compute $\nabla u_{i,j}^n$ and $F_{i,j}^n$ using the velocity field $u_{i,j}^n$.

10: Use Algorithm A.1 for $y_{i,j}^n$ to get $Z_{i,j}^{1,(p)} = (\Pi_h^{(p)} \zeta_h)(y_{i,j}^1)$.

11: Update $\zeta_{i,j}^1$ by an approximation of first order in time

$$\zeta_{i,j}^1 = [I + \Delta t(\nabla u_{i,j}^1)] Z_{i,j}^{1,(p)} [I + \Delta t(\nabla u_{i,j}^1)]^\top + \Delta t F_{i,j}^1.$$

12: **end if**

13: **end for**

14: **while** $n \leq N_T$ **do**

15: **for** $(i, j) \in \Lambda_\Omega$ **do**

16: Calculate the interpolation points $y_{i,j}^n = X_1^n(x_{i,j}) = x_{i,j} - u_{i,j}^n \Delta t$ and $\tilde{y}_{i,j}^n = \tilde{X}_1^n(x_{i,j}) = x_{i,j} - 2u_{i,j}^n \Delta t$.

17: **if** $(y_{i,j}^n \notin \bar{\Omega}$ or $\tilde{y}_{i,j}^n \notin \bar{\Omega})$ **then**

$$\zeta_{i,j}^n = \zeta_{\text{in}}^n(x_{i,j})$$

18: **else**

19: Compute $\nabla u_{i,j}^n$ and $F_{i,j}^n$ using the velocity field $u_{i,j}^n$

20: Use Algorithm A.1 for $y_{i,j}^n$ to get $Z_{i,j}^{n,(p)} = (\Pi_h^{(p)} \zeta_h)(y_{i,j}^n)$ and solve again for $\tilde{y}_{i,j}^n$ to get $\tilde{Z}_{i,j}^{n,(p)} = (\Pi_h^{(p)} \zeta_h)(\tilde{y}_{i,j}^n)$.

21: Update $\zeta_{i,j}^n$ by an approximation of second order in time

$$\begin{aligned} \zeta_{i,j}^n &= \frac{4}{3} [I + \Delta t(\nabla u_{i,j}^n)] Z_{i,j}^{n,(p)} [I + \Delta t(\nabla u_{i,j}^n)]^\top \\ &\quad - \frac{1}{3} [I + 2\Delta t(\nabla u_{i,j}^n)] \tilde{Z}_{i,j}^{n,(p)} [I + 2\Delta t(\nabla u_{i,j}^n)]^\top + \frac{2\Delta t}{3} F_{i,j}^n. \end{aligned}$$

22: **end if**

23: **end for**

24: $n \leftarrow n + 1$.

25: **end while**

Acknowledgments

D.O.M. would like to acknowledge the support of the grant 2013/07375-0 - Center of Mathematical Sciences Applied to industry (Cepid-CeMEAI), grants 2019/08742-2 and 2017/11428-2, São Paulo Research Foundation (FAPESP). H.N. is supported by JSPS KAKENHI Grant Numbers JP18H01135, JP20H01823, JP20KK0058, and JP21H04431, JST PRESTO Grant Number JPMJPR16EA, and JST CREST Grant Number JPMJCR2014. C.M.O. would like to thank the financial support of CNPq (National Council for Scientific and Technological Development) grant 305383/2019-1 and FAPESP grant 2013/07375-0.

References

- [1] M. A. Alves, P. J. Oliveira, and F. T. Pinho. Benchmark solutions for the flow of Oldroyd-b and PTT fluids in planar contractions. *Journal of Non-Newtonian Fluid Mechanics*, 110(1):45–75, 2003.
- [2] K. Baba and M. Tabata. On a conservation upwind finite element scheme for convective diffusion equations. *RAIRO. Analyse Numérique*, 15(1):3–25, 1981.
- [3] J. Baranger and A. Machmoum. Existence of approximate solutions and error bounds for viscoelastic fluid flow: Characteristics method. *Computer Methods in Applied Mechanics and Engineering*, 148(1-2):39–52, 1997.
- [4] F. G. Basombrío. Flows of viscoelastic fluids treated by the method of characteristics. *Journal of Non-Newtonian Fluid Mechanics*, 39(1):17–54, 1991.
- [5] M. Benítez and A. Bermúdez. Numerical analysis of a second-order pure Lagrange–Galerkin method for convection-diffusion problems. Part I: Time discretization. *SIAM Journal on Numerical Analysis*, 50(2):858–882, 2012.
- [6] R. Bermejo, P. Gálan del Sastre, and L. Saavedra. A second order in time modified Lagrange–Galerkin finite element method for the incompressible Navier–Stokes equations. *SIAM Journal on Numerical Analysis*, 50:3084–3109, 2012.
- [7] R. Bermejo and L. Saavedra. Modified Lagrange–Galerkin methods of first and second order in time for convection-diffusion problems. *Numerische Mathematik*, 120:601–638, 2012.
- [8] M. Breuss. The implicit upwind method for 1-d scalar conservation laws with continuous fluxes. *SIAM Journal on Numerical Analysis*, 43(3):970–986, 2005.
- [9] E. Castillo and R. Codina. Variational multi-scale stabilized formulations for the stationary three-field incompressible viscoelastic flow problem. *Computer Methods in Applied Mechanics and Engineering*, 279:579–605, 2014.
- [10] L. Chupin. Global strong solutions for some differential viscoelastic models. *SIAM Journal on Applied Mathematics*, 78(6):2919–2949, 2018.
- [11] M. Colera, J. Carpio, and R. Bermejo. A nearly-conservative, high-order, forward Lagrange–Galerkin method for the resolution of scalar hyperbolic conservation laws. *Computer Methods in Applied Mechanics and Engineering*, 376:113654, 2021.
- [12] M. S. Darwish, J. R. Whiteman, and M. J. Bevis. Numerical modelling of viscoelastic liquids using a finite-volume method. *Journal of Non-Newtonian Fluid Mechanics*, 45(3):311–337, 1992.
- [13] P. J. Dellar. Lattice boltzmann formulation for linear viscoelastic fluids using an abstract second stress. *SIAM Journal on Scientific Computing*, 36(6):A2507–A2532, 2014.

- [14] J. Douglas, Jr and T. F. Russell. Numerical methods for convection-dominated diffusion problems based on combining the method of characteristics with finite element or finite difference procedures. *SIAM Journal on Numerical Analysis*, 19(5):871–885, 1982.
- [15] M. El Hadj and P. A. Tanguy. A finite element procedure coupled with the method of characteristics for simulation of viscoelastic fluid flow. *Journal of Non-Newtonian Fluid Mechanics*, 36:333–349, 1990.
- [16] V. J. Ervin and W. W. Miles. Approximation of time-dependent viscoelastic fluid flow: SUPG approximation. *SIAM Journal on Numerical Analysis*, 41(2):457–486, 2003.
- [17] J. D. Evans, H. L. França, and C. M. Oishi. Application of the natural stress formulation for solving unsteady viscoelastic contraction flows. *Journal of Computational Physics*, 388:462–489, 2019.
- [18] R. Fattal and R. Kupferman. Constitutive laws for the matrix-logarithm of the conformation tensor. *Journal of Non-Newtonian Fluid Mechanics*, 123(5-6):281–285, 2004.
- [19] M. Fortin and A. Fortin. A new approach for the fem simulation of viscoelastic flows. *Journal of Non-Newtonian Fluid Mechanics*, 32(3):295–310, 1989.
- [20] W. Han and M. Sofonea. Evolutionary variational inequalities arising in viscoelastic contact problems. *SIAM Journal on Numerical Analysis*, 38(2):556–579, 2000.
- [21] A. Harten. On a class of high resolution total-variation-stable finite-difference schemes. *SIAM Journal on Numerical Analysis*, 21(1):1–23, 1984.
- [22] P.-Y. Hsu, H. Notsu, and T. Yoneda. A local analysis of the axisymmetric Navier–Stokes flow near a saddle point and no-slip flat boundary. *Journal of Fluid Mechanics*, 794:444–459, 2016.
- [23] M. A. Hulsen, R. Fattal, and R. Kupferman. Flow of viscoelastic fluids past a cylinder at high weissenberg number: stabilized simulations using matrix logarithms. *Journal of Non-Newtonian Fluid Mechanics*, 127(1):27–39, 2005.
- [24] H. Lee. A multigrid method for viscoelastic fluid flow. *SIAM Journal on Numerical Analysis*, 42(1):109–129, 2004.
- [25] Y.-J. Lee and J. Xu. New formulations, positivity preserving discretizations and stability analysis for non-Newtonian flow models. *Computer Methods in Applied Mechanics and Engineering*, 195(9-12):1180–1206, 2006.
- [26] Y.-J. Lee, J. Xu, and C.-S. Zhang. Global existence, uniqueness and optimal solvers of discretized viscoelastic flow models. *Mathematical Models and Methods in Applied Sciences*, 21(8):1713–1732, 2011.
- [27] Y.-J. Lee, J. Xu, and C.-S. Zhang. Stable finite element discretizations for viscoelastic flow models. In *Handbook of Numerical Analysis*, volume 16, pages 371–432. Elsevier, 2011.
- [28] M. Lukáčová-Medviděová, H. Notsu, and B. She. Energy dissipative characteristic schemes for the diffusive Oldroyd-B viscoelastic fluid. *International Journal for Numerical Methods in Fluids*, 81(9):523–557, 2016.
- [29] M. Lukáčová-Medviděová, H. Mizerová, S. Necasova, and M. Renardy. Global existence result for the generalized Peterlin viscoelastic model. *SIAM Journal on Mathematical Analysis*, 49(4):2950–2964, 2017.
- [30] M. Lukáčová-Medviděová, H. Mizerová, H. Notsu, and M. Tabata. Numerical analysis of the Oseen-type Peterlin viscoelastic model by the stabilized Lagrange–Galerkin method, Part I: A linear scheme. *ESAIM: M2AN*, 51:1637–1661, 2017.
- [31] M. Lukáčová-Medviděová, H. Mizerová, H. Notsu, and M. Tabata. Numerical analysis of the Oseen-type Peterlin viscoelastic model by the stabilized Lagrange–Galerkin method, Part II: A nonlinear scheme. *ESAIM: M2AN*, 51:1663–1689, 2017.

- [32] A. Machmoum and D. Esselaoui. Finite element approximation of viscoelastic fluid flow using characteristics method. *Computer Methods in Applied Mechanics and Engineering*, 190(42):5603–5618, 2001.
- [33] F. P. Martins, C. M. Oishi, A. M. Afonso, and M. A. Alves. A numerical study of the kernel-conformation transformation for transient viscoelastic fluid flows. *Journal of Computational Physics*, 302:653–673, 2015.
- [34] J. Málek, V. Průša, T. Skřivan, and E. Süli. Thermodynamics of viscoelastic rate-type fluids with stress diffusion. *Physics of Fluids*, 30(2):023101, 2018.
- [35] H. Notsu, H. Rui, and M. Tabata. Development and L^2 -analysis of a single-step characteristics finite difference scheme of second-order in time for convection-diffusion problems. *Journal of Algorithms & Computational Technology*, 7:343–380, 2013.
- [36] H. Notsu and M. Tabata. Error estimates of a pressure-stabilized characteristics finite element scheme for the Oseen equations. *Journal of Scientific Computing*, 65(3):940–955, 2015.
- [37] H. Notsu and M. Tabata. Error estimates of a stabilized Lagrange–Galerkin scheme for the Navier–Stokes equations. *ESAIM: M2AN*, 50(2):361–380, 2016.
- [38] H. Notsu and M. Tabata. Stabilized Lagrange–Galerkin schemes of first-and second-order in time for the Navier–Stokes equations. In *Advances in Computational Fluid-Structure Interaction and Flow Simulation*, pages 331–343. Springer, 2016.
- [39] J. G. Oldroyd. On the formulation of rheological equations of state. *Proceedings of the Royal Society of London. Series A. Mathematical and Physical Sciences*, 200(1063):523–541, 1950.
- [40] P. J. Oliveira and A. I. Miranda. A numerical study of steady and unsteady viscoelastic flow past bounded cylinders. *Journal of non-newtonian fluid mechanics*, 127(1):51–66, 2005.
- [41] P. J. Oliveira, F. T. Pinho, and G. A. Pinto. Numerical simulation of non-linear elastic flows with a general collocated finite-volume method. *Journal of Non-Newtonian Fluid Mechanics*, 79(1):1–43, 1998.
- [42] J. Petera. A new finite element scheme using the Lagrangian framework for simulation of viscoelastic fluid flows. *Journal of Non-Newtonian Fluid Mechanics*, 103(1):1–43, 2002.
- [43] F. Pimenta and M. A. Alves. Stabilization of an open-source finite-volume solver for viscoelastic fluid flows. *Journal of Non-Newtonian Fluid Mechanics*, 239:85–104, 2017.
- [44] O. Pironneau and M. Tabata. Stability and convergence of a Galerkin-characteristics finite element scheme of lumped mass type. *International Journal for Numerical Methods in Fluids*, 64:1240–1253, 2010.
- [45] M. Renardy. Mathematical analysis of viscoelastic flows. *Annual review of fluid mechanics*, 21:21–36, 1989.
- [46] M. Renardy. An existence theorem for model equations resulting from kinetic theories of polymer solutions. *SIAM Journal on Mathematical Analysis*, 22(2):313–327, 1991.
- [47] M. Renardy. *Mathematical analysis of viscoelastic flows*. SIAM, 2000.
- [48] H. Rui and M. Tabata. A second order characteristic finite element scheme for convection-diffusion problems. *Numerische Mathematik*, 92:161–177, 2002.
- [49] D. Sandri. Finite element approximation of viscoelastic fluid flow: existence of approximate solutions and error bounds. continuous approximation of the stress. *SIAM Journal on Numerical Analysis*, 31(2):362–377, 1994.
- [50] A. Schlichting and C. Seis. Convergence rates for upwind schemes with rough coefficients. *SIAM Journal on Numerical Analysis*, 55(2):812–840, 2017.

- [51] E. Süli. Convergence and nonlinear stability of the Lagrange–Galerkin method for the Navier–Stokes equations. *Numerische Mathematik*, 53:459–483, 1988.
- [52] M. Tabata. Discrepancy between theory and real computation on the stability of some finite element schemes. *Journal of Computational and Applied Mathematics*, 199:424–431, 2007.
- [53] M. Tabata and S. Fujima. Robustness of a characteristic finite element scheme of second-order in time increment. In C. Groth and D. Zingg, editors, *Computational Fluid Dynamics 2004*, pages 177–182. Springer, 2006.
- [54] M. Tabata and S. Uchiumi. A genuinely stable Lagrange–Galerkin scheme for convection-diffusion problems. *Japan Journal of Industrial and Applied Mathematics*, 33:121–143, 2016.
- [55] M. Tabata and S. Uchiumi. An exactly computable Lagrange–Galerkin scheme for the Navier–Stokes equations and its error estimates. *Mathematics of Computation*, 87(309):39–67, 2018.
- [56] M. F. Tomé, N. Mangiavacchi, J. A. Cuminato, A. Castelo, and S. Mckee. A finite difference technique for simulating unsteady viscoelastic free surface flows. *Journal of Non-Newtonian Fluid Mechanics*, 106(2-3):61–106, 2002.
- [57] J. Venkatesan and S. Ganesan. A three-field local projection stabilized formulation for computations of Oldroyd-B viscoelastic fluid flows. *Journal of Non-Newtonian Fluid Mechanics*, 247:90–106, 2017.
- [58] K. Walters and M. Webster. The distinctive cfd challenges of computational rheology. *International journal for numerical methods in fluids*, 43(5):577–596, 2003.
- [59] J. L. White. Dynamics of viscoelastic fluids, melt fracture, and the rheology of fiber spinning. *Journal of Applied Polymer Science*, 8(5):2339–2357, 1964.
- [60] H. C. Yee, G. H. Klopfer, and J.-L. Montagne. High-resolution shock-capturing schemes for inviscid and viscous hypersonic flows. *Journal of Computational Physics*, 88(1):31–61, 1990.